Available online at www.sciencedirect.com
SCIENCE DIRECT®
Composites Science and Technology 65 (2005) 2344–2363
COMPOSITES SCIENCE AND TECHNOLOGY
www.elsevier.com/locate/compscitech

Polymer nanocomposite foams

L. James Lee *, Changchun Zeng, Xia Cao, Xiangming Han, Jiong Shen, Guojun Xu

Department of Chemical and Biomolecular Engineering, The Ohio State University, Columbus, OH 43210, USA

Received 9 April 2005; received in revised form 21 June 2005; accepted 22 June 2005
Available online 19 August 2005

Abstract

Polymer nanocomposite foams have received increasingly attention in both scientific and industrial communities. The combination of functional nanoparticles and supercritical fluid foaming technology has a high potential to generate a new class of materials that are lightweight, high strength and multifunctional. A small amount of well-dispersed nanoparticles in the polymer domain may serve as the nucleation sites to facilitate the bubble nucleation process. Moreover, the nano-scaled particles are suitable for micro-scaled reinforcement, thus achieving the macroscopic mechanical enhancement. In this paper, we will first briefly review the synthesis and processing techniques of nanocomposites based on polymers that are important in the foam industry. Both thermoplastic and thermoset nanocomposite foams will be addressed. This is followed by an introduction of various foaming techniques. The effect of nanoparticles on the foam morphology and properties is then discussed. We conclude with the current and future trends of nanocomposite foams in both industrial and biomedical applications.

Keywords: Polymer nanocomposite; Nanocomposite foam; Nucleation; Bubble growth; Cell size; Cell density

1. Introduction

Polymer nanocomposites have drawn a great deal of interest in recent years because these materials possess high potential to achieve great property improvement by adding a small amount of nanoparticles in the polymer matrices. Plastic foams, on the other hand, represent a group of lightweight materials that have been widely used in a variety of industries with a market value of US $2 billion in 2000. However, the foam applications are limited by their inferior mechanical strength, poor surface quality, and low thermal and dimensional stability. Furthermore, the most widely used chlorofluorocarbon (CFC) blowing agents have been found to cause ozone depletion in the upper atmosphere and will be banned by 2010, according to the Montreal Protocol. Environmentally benign gases such as supercritical carbon dioxide ($ScCO_2$) are attractive alternatives for CFCs as blowing agents. But low solubility and high diffusivity of CO_2 in polymers make it more difficult to control the foam morphology. A small amount of well-dispersed nanoparticles in the polymer may serve as nucleation sites to facilitate the bubble nucleation process. Plate-like nanoparticles can also reduce gas diffusivity in the polymer matrix. In addition, the presence of nanoparticles may enhance mechanical and physical properties, the heat distortion temperature, and fire resistance of polymer foams. Novel nanocomposite foams based on the combination of functional nanoparticles and supercritical fluid foaming technology may lead to a new class of materials that are ligh weight, high strength and multifunctional. In this article, we review the recent progress in this area.

Polymer nanocomposites cover a vast array of different polymer matrices and nanoparticles. A detailed survey on this topic is beyond the scope of this paper. The readers are referred to dedicated reviews for details [1–6]. We will first briefly review the synthesis and processing techniques

* Corresponding author. Tel.: +1 614 292 2408; fax: +1 614 292 3769.
E-mail address: lee.31@osu.edu (L.J. Lee).

0266-3538/$ - see front matter © 2005 Elsevier Ltd. All rights reserved.
doi:10.1016/j.compscitech.2005.06.016

of nanocomposites based on polymers that are important in the foam industry. Both thermoplastic and thermoset nanocomposite foams will be addressed. This is followed by an introduction of foaming processing methods. The effect of nanoparticles on the foam morphology and properties is then discussed. We conclude with current and future trends of nanocomposite foams in both industrial and biomedical applications.

1.1. Polymer nanocomposites

Polymer composites are widely used in automotive, aerospace, construction, and electronic industries because they provide improved mechanical properties (e.g., stiffness, strength) and physical properties over pure polymers. Micron-sized particulates and long fibers are most widely used in traditional polymer composites. Nanocomposites are a new class of materials providing superior properties when compared to their microcomposite counterparts. An addition of a small amount of nanoparticles can significantly improve a variety of properties without sacrificing the lightweight of polymer matrices.

Nanocomposites usually refer to composites in which at least one phase (the filler phase) possesses ultrafine dimensions (on the order of a few nanometers). They include the use of three different types of nanoparticles as shown in Fig. 1. The first type of nanoparticles only has one dimension in the nanometer scale. They possess a platelet-like structure. The lateral dimension may be in the range of several hundred nanometers to microns, while the thickness is usually less than a few nanometers. Clay is a good example of this type of nanoparticle. Layered nanographites are another example. If two dimensions of the nanoparticles are at the nanometer scale while the third is larger, these particles possess an elongated structure. Nanotubes and nanofibers belong to this group. The third type of nanoparticle has all three dimensions at the nanometer scale; for example, spherical silica particles, nanocrystals, gold and other metal nanoparticles, and block copolymers. A variant of this type of particle is the nanoporous microparticles. While the diameter of the particle may be in the order of microns, the pore sizes are in the order of nanometers. While all three types of nanoparticles have been used in nanocomposite synthesis and processing, plate-like clay nanoparticles and fiber/tube like carbon nanofibers (CNFs) and carbon nanotubes (CNTs) have attracted the most attention. The nanocomposites and nanocomposite foams discussed in this article are mainly based on these nanoparticles.

1.2. Polymer foams

Foams are defined as materials containing gaseous voids surrounded by a denser matrix, which is usually a liquid or solid. Foams have been widely used in a variety of applications: e.g., insulation, cushion, absorbents and weight-bearing structures [7]. Foams of high porosity with interconnected pores have also been used as tissue engineering scaffolds for cell attachment and growth [8]. Various polymers have been used for foam applications, e.g., polyurethane (PU), polystyrene (PS), polyolefin (polyethylene (PE) and polypropylene (PP)), poly(vinyl chloride) (PVC), polycarbonate (PC), just name a few. Table 1 [9] displays the US market for polymer foams by resin family in 2001 and 2006, and the projected growth rate for each resin family.

In 2001, the US use of polymer foam products was 7.42 billion pounds and that transfers into a $16.2 billion market [10]. PU occupies the largest market share (53%) in terms of the amount consumed, while PS is the second (26%).

Depending on the composition, cell morphology and physical properties, polymer foams can be categorized as rigid or flexible foams. Rigid foams are widely used in applications such as building insulation, appliances, transportation, packaging, furniture, flotation and cush-

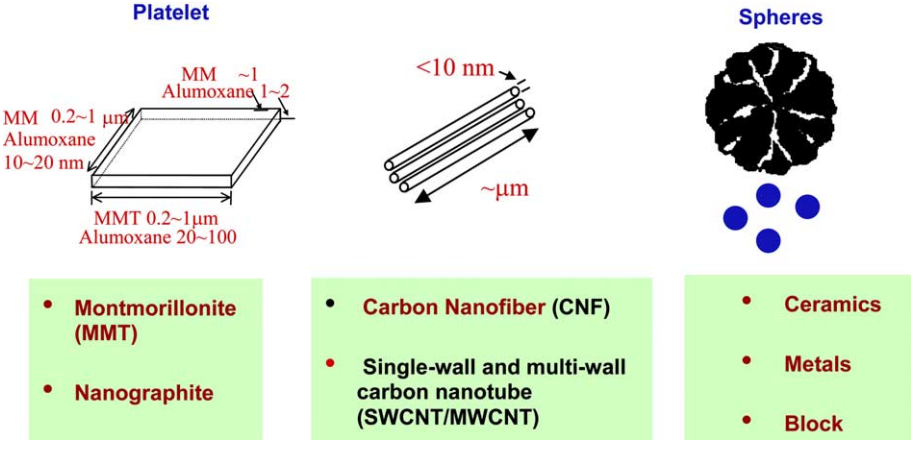

Fig. 1. Different nanoparticles.

Table 1
US market for polymeric foams by resin family, through 2006 (million lbs.)

Polymer	Year		Average annual growth rate (%)
	2001	2006	
PU	3961	4720	3.6
PS	1913	2031	1.2
PVC	1156	1315	2.6
Polyolefin	300	361	3.8
Others	91	102	2.3
Total	7421	8529	2.8

ion, and food and drink containers, whereas flexible foams are used as furniture, transportation, bedding, carpet underlay, textile, gaskets, sports applications, shock and sound attenuation, and shoes.

According to the size of the foam cells, polymer foams can be classified as macrocellular (>100 μm), microcellular (1–100 μm), ultramicrocellular (0.1–1 μm) and nanocellular (0.1–100 nm).

Polymer foams can also be defined as either closed cell or open cell foams. In closed cell foams, the foam cells are isolated from each other and cavities are surrounded by complete cell walls. In open cell foams, cell walls are broken and the structure consists of mainly ribs and struts. Generally, closed cell foams have lower permeability, leading to better insulation properties. Open cell foams, on the other hand, provide better absorptive capability.

2. Synthesis of nanocomposite foams

One-step reactive foaming is typical for thermoset polymers. A good example is PU/clay nanocomposite foams [11,12], where a physical blowing agent such as pentane is mixed with monomers and clay nanoparticles. Reaction exotherm leads to a temperature jump and foaming. Most thermoplastic nanocomposite foams to date are synthesized via a two-step process: the nanocomposite is synthesized first and followed by foaming. We shall briefly review the two steps separately.

2.1. Nanocomposite synthesis

The goal of the synthesis of nanocomposites is to achieve controlled nanoparticle dispersion and distribution in a polymer matrix. This is not a trivial task and is still a largely unaccomplished task. For example, each individual clay platelet offers a large surface area and high aspect ratio, and both are critical for improving mechanical properties, thermal stability and barrier properties. However, typical clay particles contain a large number of crystallites. The crystallite itself contains hundreds of individual layers stacking together. A typical clay particle may contain several thousand individual layers. Separating and distributing these layers throughout polymer matrices require the development of special surface chemistry, and dedicated synthesis and processing technologies. The most widely used strategy is to bind surfactants onto the clay surface in order to increase the hydrophobicity and compatibility through ion exchange reactions with the polymer matrices [1,2,13] . Studies on polymer-CNTs and polymer-CNFs composites also show that CNTs/CNFs are inclined to hold together as bundles and ropes in the polymer matrix due to the intrinsic van der Waals attraction [14–16]. Strategies proposed to accomplish good dispersion include the use of ultrasonication, high shear mixing, surfactants, and functionalization of the carbon surface [14,17–21].

Typically, three approaches have been adopted to synthesize polymer nanocomposites: solution blending, melt blending, and in situ polymerization. In solution blending, a solvent or solvent mixture is used to disperse the nanoparticles and dissolve the polymer matrix. Depending on the interactions of the solvent and nanoparticles, the nanoparticle aggregates can be disintegrated in a good solvent due to the weak van der Waals force that stacks the layers together. Polymer chains can then be adsorbed onto the nanoparticles. However, upon solvent removal, the nanoparticles tend to re-agglomerate. Few exfoliated nanocomposites were prepared via this method. Another disadvantage of this method is the large amount of solvent needed, resulting in a high product cost. The types of polymers that can be used to sythesize nanocomposites ultimately depend on the selection of proper solvent, limiting the applicability of this method. Nevertheless, this is an attractive route to prepare nanocomposites based on water soluble polymer and layered silicate nanocomposites because most water soluble polymers are polar and hydrophilic enough to interact with the silicate surface without the need of cation exchange modification on the silicate surface. It is well known that inorganic layered silicates are able to exfoliate in water and form colloidal particles. Several polymer nanocomposites, including polyethylene oxide (PEO) [22], polyvinyl alcohol (PVA) [23], and polyacrylic acid (PAA) [24] were prepared via this method. Some polymer/CNFs nanocomposites are also synthesized by this method [20,25].

Instead of using solvent as the medium, nanoparticles can be directly mixed with a molten polymer. This process eliminates the use of solvent and is compatible with industrial polymer extrusion and blending processes. It offers an economically attractive route in fabricating polymer nanocomposites. A wide variety of polymer/clay nanocomposites have been prepared via this route, i.e., nylon 6 [26–30], PS [31–34], and PP [35–42]. Melt intercalation offers a 'simple' way of preparing nanocomposites. However, care has to be taken to 'fine tune' the layered silicates surface chemistry in order to

increase the silicate compatibility with the polymer matrix. Many studies have shown that the polar interactions of polymer and clay surface play a critical role in achieving particle delamination/dispersion [43–46]. For non-polar polymers, e.g., PP, a polar compatibilizer such as maleic anhydride modified PP (PP-MA) is commonly added to improve the compatibility of PP and clay and thus the clay nanoparticle dispersion. All reported studies on PP nanocomposite foams were synthesized in this manner. Processing conditions such as shear rate and mixing have profound effects on the structure evolution of polymer nanocomposites by melt intercalation and these effects are still not well understood [28]. Polymer/CNFs nanocomposites have also been synthesized via this method [47–49]. Shear stress is extremely important to disintegrate and disperse nanoparticles, therefore it needs to be controlled at an appropriate level. Too strong a shear force tends to break single fibers into many shorter pieces [50] reducing the reinforcement efficiency and deteriorating properties in which high aspect ratio of the nanoparticle is essential.

Unlike melt intercalation, layered silicates is mixed with monomer before polymerization takes place in in situ polymerization. Because of the low monomer viscosity (comparing to melt viscosity), it is much easier to achieve uniform mixing of particles in the monomer using a high shear mixer. In addition, the low viscosity and high diffusivity result in a higher rate of monomer diffusion into the interlayer region. It is also possible to control nanocomposite morphology through the combination of reaction conditions and clay surface modification. For most thermoset polymers, in situ polymerization is the only viable method to prepare nanocomposites. By tailoring the interactions between the monomer, the surfactant, and the clay surface, exfoliated nanocomposites (e.g., nylon-6 [51], poly(ε-caprolactone) [52], epoxy [53] and polycarbonate [54]) have been successfully synthesized via the ring-opening polymerization. The functional group in the organic cation can catalyze the intralayer polymerization and facilitate layer separation. Free radical polymerization has also been employed to synthesize many thermoplastic nanocomposites. Efforts have been made to anchor initiators in the interlayer region to improve the intralayer polymerization rate for exfoliated nanocomposites [55]. Reactive groups containing carbon-carbon double bonds were introduced to the clay surface via several approaches [56–58]. Clay exfoliation/delamination has been dramatically enhanced this way. In our laboratory, a nanoclay was prepared by the ion exchange of a reactive cationic surfactant, 2-methacryloyloxyethylhexadecyldimethyl-ammonium bromide (MHAB, structure shown in Fig. 2) with cations on the montmorillonite surface. Compared to a commercial nanoclay, Closite 20A from Southern Clay, which contains a non-polar aliphatic chain with a similar length, the anchored organic surfactant with polymerizable groups on MHABS provides an additional kinetic driving force for layer separation. The TEM micrograph (Fig. 2(a)) of the intercalated PS/20A nanocomposite demonstrates that large clay aggregates are still present in the matrix. Face-to-face layer stacking and low angle intergrowth of tactoids is still observable. A TEM micrograph of PS/MHABS is shown in Fig. 2(b). The tactoids have been completely delaminated and uniformly dispersed in the matrix. Most clay layers are present as single layers, while stacks of a few layers are also observable in some region. Near complete exfoliation was reported for PS nanocomposites synthesized with this reactive nanoclay at a clay concentration of 20 wt% [59].

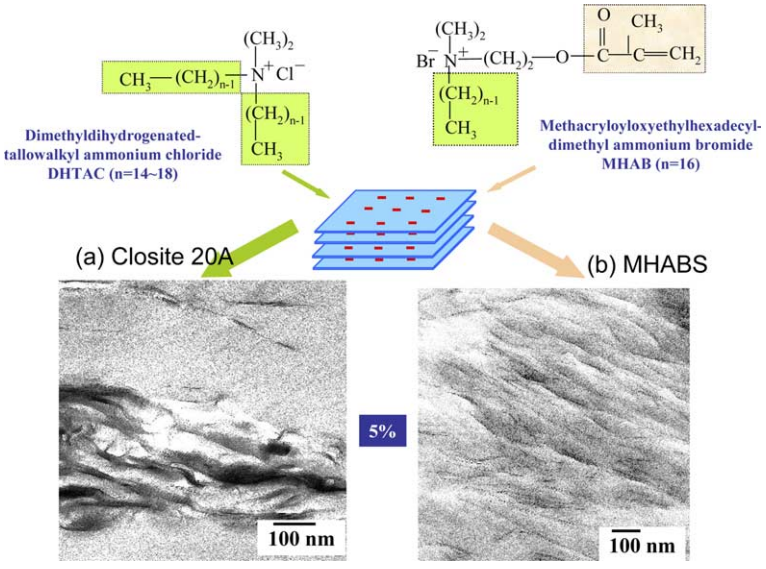

Fig. 2. Intercalated and exfoliated PS/clay nanocomposites.

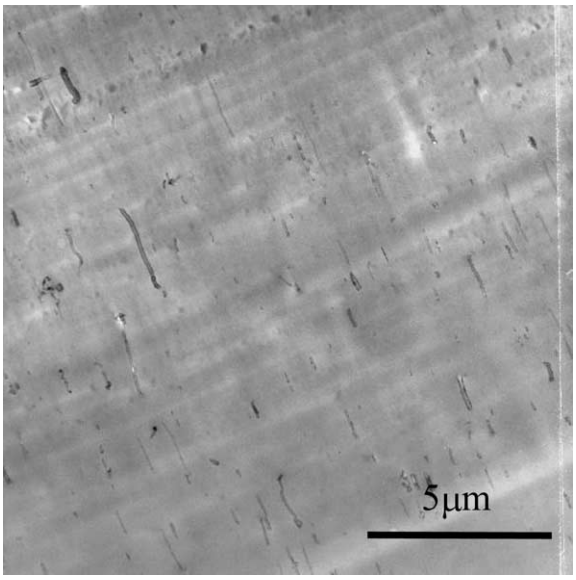

Fig. 3. TEM image of PS/1 wt% CNF nanocomposite.

CNTs/CNFs nanocomposites have also been synthesized via in situ polymerization [60–62]. The system viscosity needs to be high enough in order to fix the fibers in the monomer phase in the early stage of polymerization. Otherwise, CNFs would be inclined to bind with each other, causing a reduction of particle dispersion and other physical properties. Fig. 3 shows a complete dispersion of CNFs (the dark lines) in the PS matrix. Here, 10 wt% of PS was added into the mixture of styrene/CNFs to achieve a higher initial viscosity and consequently a more stable fiber suspension. In the case of PS/CNTs nanocomposites, the dispersion of carbon nanotubes is not easy. The same shear mixing and ultrasonication used to disperse 1%wt CNFs was not enough to separate 0.1% CNTs aggregates in styrene [63].

PS, PVC and polyolefins are the three primary thermoplastics used in polymer foams. Synthesis of nanocomposites based on these three polymers is briefly introduced next.

2.1.1. Synthesis of PS nanocomposites

PS/clay nanocomposites were synthesized in both intercalated and exfoliated structures [58,64,65]. To prepare the nanocomposites, organo-nanoclay particles are pre-mixed with PS and then mechanically blended in single or twin-screw extruders. The formation of nanocomposites relies on the penetration of polymer chains into the interlayer region to separate the layers. The layer separation depends on the establishment of favorable interactions between the polymer and the clay surface and the subsequent system energy reduction. Limited interactions resulted in limited polymer chain penetration, leading to intercalated nanocomposites [31–34,58,64,65].

In situ polymerization has also been carried out to prepare PS nanocomposites. By using reactive surfactants, the copolymerization of the interlayer surfactant and styrene monomer provides the driving force for delamination of clay crystallite. Highly exfoliated PS/clay nanocomposites have been formed this way [55,58,64–71].

2.1.2. Synthesis of PVC nanocomposites

PVC is a widely used matrix material in thermoplastic foams. Some efforts have been devoted to develop PVC nanocomposites for improved PVC properties [72–84]. Particles used include clay, calcium carbonate, hydrosulfite, copper, and antimony trioxide [81–83,85]. The polar nature of the C–Cl bond makes it possible to form exfoliated nanocomposites of PVC in melt blending [77,80,86–89]. However, clay surface modification is usually needed to achieve exfoliation [76,86]. For example, exfoliated PVC nanocomposites have been realized by melt blending when the clay was modified by aromatic amine [77]. However, melt processing of PVC with alkyl-modified clays only produced partially exfoliated nanocomposites [77]. A plasticizer like dioctylphalate (DOP) may serve as a co-intercalate to increase clay dispersion in PVC [90,91]. In situ polymerization of PVC/clay nanocomposoites has been carried out by either emulsion polymerization or suspension polymerization [72,76,79,92]. In general, in situ polymerization methods can achieve a much better clay dispersion. Highly exfoliated PVC/clay nanocomposites can also be produced by flocculating a mixture of polymer and clay mineral dispersions [93] or by solution blending [94]. However, organoclay tends to induce the degradation of PVC because of its low thermal stability. The allylic and tertiary chlorines of PVC chains are the main labile sites to release hydrogen chloride. When the mass loss due to dehydrochlorination reaches 0.1%, sequences of conjugated double bonds form, resulting in discoloration of PVC by the zipelimination mechanism [95]. In PVC nanocomposites, the quaternary ammonium salts used for clay modification may accelerate the degradation of PVC [73,96]. The organic ammonium cations act as Lewis acid, causing chlorine ions to separate from the PVC matrix and to release HCl [77]. Several approaches can be used to reduce or eliminate PVC degradation when processed with nanoclay. One approach is to co-intercalate DOP into organoclay and then compound the mixture with PVC. DOP covers the quaternary amine groups preventing the contact between amine and active chloride atoms [97,98]. Another approach is to intercalate/exfoliate nanoclay in a polymer, such as epoxy or poly caprolactone (PCL) [99,100] which has good miscibility with PVC, by in situ polymerization. The clay surface is protected by a layer of epoxy or PCL to prevent the direct contact with PVC in melt blending, inhibiting its degradation.

2.1.3. Synthesis of polyolefin nanocomposites

Polyolefin represents a large group of thermoplastic polymers. Melt intercalation usually results in immiscible microcomposites. This is because polyolefin is very nonpolar and hydrophobic while clay is highly hydrophilic. The enthalpic barrier prevents the intercalation of polymer chains [43–46]. In melt intercalation, usually a third functionalized ingredient is added to serve as the compatibilizer in order to improve the compatibility of polyolefin and clay surface. In situ polymerization of polyolefins in the presence of clay has been conducted by several research groups. Tudor et al. [101] used a synthetic fluorohectorite to prepare PP nanocomposites. In their study, a cationic metallocene catalyst was incorporated into the gallery region to catalyze propylene polymerization. Another cationic palladium based catalyst was incorporated in 1-tetradecylammonium cations modified synthetic fluorohectorite. This complex can catalyze ethylene polymerization at high yield, producing exfoliated nanocomposites [102]. Exfoliated PE nanocomposites were also prepared using metallocene catalyst [103]. However, the formed nanocomposite is not thermodynamically stable. During melt processing, the exfoliated structure tends to collapse into an intercalated structure.

2.2. Synthesis of thermoplastic nanocomposite foams

The synthesized nanocomposites can be used to produce nanocomposite foams. For large-scale production, the direct utilization of foaming (blowing) agents is the most commonly used method. Foaming agents are substances that form the gaseous phase in the foams. Two types of foaming agents are often used: physical or chemical blowing agents. Chemical foaming agents are usually reactive species that produce gases in the foaming process, while physical foaming agents are substances that gasify under foaming conditions. Typical physical foaming agents are volatile chemicals such as chlorofluorocarons (CFC), volatile hydrocarbons and alcohols, or inert gases such as nitrogen, carbon dioxide, argon, and water. Foams can be produced in either the liquid/melt state by extrusion, injection molding or compression molding, or the solid state where gas is forced into a solid polymer followed by depressurization. Both methods can use either physical or chemical blowing agents.

In addition to utilizing a blowing agent, porous polymeric materials can also be prepared by other methods such as phase inversion, leaching [104] and thermal decomposition [105]. Most of these methods are only suitable for preparation of thin film products. We will focus on the foaming processes utilizing foaming/blowing agents. In physical foaming, a blowing gas is first dissolved in the polymer to form a homogeneous mixture. This is usually done through pressurization. Subsequent pressure release or temperature increase results in a supersaturation state, and gas starts to form nuclei and expand. The traditional CFC physical blowing agents have good solubility in the polymer matrix, low diffusivity and low thermal conductivity that result in foam products with good insulation and physical properties. However, their use has been greatly reduced globally because of their high ozone depletion effect. In recent years, the foam industry has switched to blowing agents containing less chlorine atoms by replacing them with hydrogen and fluorine atoms (i.e., HCFCs).

The HCFCs are hydrogen-containing chlorofluorocarbons such as HCFC-141b (CCl2FCH3), HCFC-142b (CF2ClCH3), and HCFC-22 (CHF2Cl) that have lower ozone-depletion potential (ODP). North America (United States and Canada) is currently using HCFC-142b (CH3-CF2Cl2) for extruded polystyrene (XPS) foam production. HCFCs will be phased out by 2010. Other choices of foam blowing agents include hydrofluorocarbon HFCs such as HFC-134a (CH2F-CF3) and HFC-152a (CH3-CHF2); hydrocarbons (propane, butane, pentane, etc.); inert gases such as nitrogen, argon and CO_2; and water. HFCs do not destroy the ozone, but they have a negative impact on global warming and their applications will most likely be regulated in the near future. Hydrocarbons present some serious problems, such as a greater fire hazard in closed-cell foams due to the entrapped blowing agent as well as adding to VOC emissions. Precaution must be taken to ensure safety of utilizing alkynes, which can be explosive in production. Among the rest, CO_2 is the most favorable choice because it is inexpensive, non-toxic, and environmentally benign (zero Ozone Depletion Potential, and 100 year Global Warming Potential compared to 1300 years for HFC-134a and 2000 years for HCFC-142b) [106].

Many challenges must be met to enable the use of CO_2 as a blowing agent. The three primary issues are: (1) The low solubility of CO_2 in most polymer melts – for instance, the solubility of CO_2 in PS is only about 3.5% at 150 °C and 10 MPa pressure; however, a solubility of 5–6% is required to achieve the necessary cell growth. (2) CO_2 has a high diffusivity in the polymer melt due to its small size – while this ensures a fast mixing process, it also results in quick escape of gas from the foam after processing. (3) CO_2 has a higher gas thermal conductivity in comparison with that of HFC blowing agents. Blending CO_2 with other hydrocarbons, such as CO_2/2-ethyl hexane and CO_2/ethanol leads to solubility similar to HCFCs, but this suffers from the same drawbacks of hydrocarbons. Nanocomposites offer several potential advantages in the foaming processes. The surface of nanoparticles can be modified to increase intermolecular interactions with CO_2. The plate-like nanoparticles can improve the barrier property by slowing down the CO_2 diffusion. Nanoparticles may also enhance the nucleation rate in the foaming process.

Microcellular foams, which are characterized by foams with cell size less than 10 μm and cell density higher than

10^9 cells/cm^3, have shown many promising properties compared to conventional foams, which usually have a cell size around 100 μm and cell density less than 10^6 cells/cm^3. But they require very stringent conditions to produce, e.g., extremely high pressure and high pressure drop rate. This greatly limits the processing window and the attainable size of the foam products. The presence of nanoparticles may overcome this bottleneck.

2.2.1. Non-continuous foaming

Foams can be produced by both non-continuous processes, e.g., batch foaming, injection molding foaming, and continuous processes such as extrusion foaming. In a batch foaming process, materials are first saturated with the foaming agent under certain temperatures and pressures. If the temperature is higher than the glass transition temperature, T_g, of the polymer matrix, the release of pressure would result in supersaturation and cell nucleation and growth. Cell structure is usually fixed by cooling the materials below its T_g. When the saturation temperature is lower than T_g, the cell is not able to nucleate and grow after the release of pressure even if gas is in the supersaturation state because of the glassy nature (high rigidity) of the matrix. Foaming may occur when temperature is raised above T_g. Cell structure is again fixed by cooling. The latter method allows independently manipulate saturation and the foaming condition, leading to higher process flexibility. However, during the transfer of gas-saturated materials to the high temperature environment, diffusion would inevitably occur, leading to a thick skin region. The major factors that determine the cell density are the saturation temperature, pressure, and pressure drop rate, and in the latter case, the temperature jump rate. Batch foaming is usually carried out at temperatures far below the polymer flowing temperature. The saturation time is very long (from hours to days depending on diffusivity). This greatly limits the productivity. Recently, a semi-continuous process was developed [107]. In this process, a roll of polymer sheet with a gas channeling material (a flexible and highly permeable material) interleaved between the layers of polymers is saturated in a pressurized chamber with the foaming gas, usually under room temperature. Pressure is then released. The saturated polymer roll is then separated from the channeling material and pulled through a heating station to foam the polymers. This technique is similar to the second batch foaming method mentioned above (the saturation temperature is lower than T_g, but foaming occurs when temperature is raised above T_g) but can yield higher productivity. The majority of studies on nanocomposite foams were conducted via batch foaming. Polymers used include PS [64,108,109], PP [110,111], PLA [112,113], PC [114], and PVC [115].

Batch foaming of expanded plastics were also investigated. Expanded polypropylene (EPP) is comprised of thermoplastic PP and an embedded low-boiling hydrocarbon compound as a blowing agent. When heated, there is an increase in the volume due to vaporization of the blowing agent. EPP is used for wings and fuselages for combat flying or in automotive applications (e.g., bumpers, dashes, etc.), that require effective impact energy absorption [116]. It is also widely used in building, transport containers and packaging components [117]. The foams made by EPP beads can bond together, essentially presenting a closed cellular structure. They exhibit greater strength and multi-cycle impact durability than other polymer foams. Because of its thermoplastic nature, EPP facilitates re-use of scrap and recycling after use. Its low density helps meet impact requirements using less material. Expandable polystyrene (EPS) foams are also studied and widely used as insulation materials in building [116,118]. Most ordinary white coffee cups and packaging foams are examples of EPS. Expanded-bead foam is unsuitable for structural core material due to its poor mechanical properties.

Compared with the extrusion foaming process, foam injection molding has its own advantages to produce parts with complex geometry. Currently, foam injection molding using CO_2 as the foaming agent is applied to produce lightweight products with high mechanical strength. MuCell molding technology, invented by Suh et al. [119], has been successfully commercialized by Trexel [120,121] to injection mold microcellular foams after a series of modifications on certain components of a standard reciprocating-screw injection molding machine, such as the plasticizing unit, injection unit, hydraulic unit, clamping unit, and gas delivery unit. To produce microcellular foams, a new screw designed for better mixing and a new sealed barrel with gas injectors were used. The injection unit requires a fast injection speed to achieve the high pressure drop rate. It was found that a finer cell structure and more uniform cell size distribution can be achieved by controlling the pressure drop rate at the mold gate than at the injection nozzle. Of course, the injection speed should be controlled below the shear limit to prevent the melt fracture. Generally, foaming injection molding achieves increased melt flowability, smaller shot size, lower injection pressures, faster cycle times, and greater dimensional stability and weight savings in molded parts [122,123].

Nylon 6/clay nanocomposite microcellular foams were foamed on an injection-molding machine equipped with a commercially available supercritical fluid (SCF) system [124,125]. The results show that microcellular nanocomposite samples exhibit smaller cell size and uniform cell distribution as well as higher tensile strength compared to the corresponding base PA-6 microcellular samples. Among the molding parameters studied, shot size has the most significant effect on cell size, cell density, and tensile strength. The minimum cell size was achieved at the medium shot size. Conceivably, the larger the shot size, the slower the cooling rate, and thus the longer the cooling

time promotes more cell growth. On the other hand, with the smaller shot size, the cells have more space to grow, which is in favor of larger cell sizes. When the same shot size is used or the same amount of material is injection molded, the finer and denser microcells in samples usually lead to higher impact strength and less reduction in tensile strength, unless some defects such as coalescence and open cells occur in the cell formation. PP/clay nanocomposites were also foamed via the MuCell process [126].

2.2.2. Continuous foaming

Continuous extrusion foaming is the most commonly used technology in the foam industry. Both single- and twin-screw extruders can be used for plastic foaming. In a typical extrusion foaming process [10], the foaming gas is first injected into the barrel and mixed with the polymer to form a homogenous solution. When the homogenous polymer/gas mixture passes through a die, a rapid pressure drop induces phase separation and cell nucleation. Pressure drop, and especially the pressure drop rate, is the primary driving force for cell nucleation [127]. An extra shaping die is used to control the product shape and foam expansion. The foamed materials continue to expand until the extrudate temperature is lower than T_g and the foam product is vitrified. Extrusion foaming of PS/clay was conducted with both intercalated and exfoliated nanocomposites using CO_2 as the foaming agent [65]. The effects of processing parameters, i.e., mass flow rate and pressure drop rate on the foam morphology, have been investigated. Due to the viscosity increase in the nanocomposites, a higher pressure drop rate is realized with the use of nanocomposites under the same processing conditions, thus greatly enhancing the nucleation rate. Extrusion foaming of PS/CNFs nanocomposite has also been reported recently [50].

2.3. Synthesis of thermoset nanocomposite foams

There are far fewer studies on thermoset nanocomposite foams than thermoplastics counterparts. Most literatures are concerned with PU nanocomposite foams [11,12,128–136]. Some are related to polyisocyanurate [130] and phenolic nanocomposite foams [137]. Several patents on PU nanocomposite foams claim significant property improvement, such as improved compressive strength [129], thermal insulation [130], and fire retardance [131]. However, few details were provided in the literature.

To prepare thermoset nanocomposite foams, nanoparticles are first dispersed uniformly in one or more monomers. The mixture is then foamed by adding other monomers. Foaming agents could be either physical or chemical blowing agents. Similar to the synthesis of thermoplastic nanocomposites, the surface modification of nanoparticles is essential for nanoparticle dispersion. In most studies, the layered silicates were modified with functional surface modifiers that can react with one of the reactants to form an intermediate leading to a uniform nanoparticle distribution in the polymer matrix during foaming.

3. Morphology and properties

Two basic steps are involved in the foaming process: bubble nucleation and growth. Nucleation is the process in which a new phase (bubble phase) is generated from the initially homogeneous polymer-gas mixture. Growth is the process in which bubble nuclei grow into final bubbles. Both processes are affected by many physical properties such as viscosity, gas solubility, surface tension, and glass transition temperature. To make things more complicated, these properties are inter-related and many are complex functions of foaming conditions (temperature and pressure).

Nucleation is a classical phenomenon and it exists in many processes, e.g., vapor condensation and crystallization. During nucleation, molecules overcome an energy barrier and gather together (via the local density and energy fluctuation) to form embryos of the new phase. When the sizes of the embryos are smaller than a critical size, an increase of embryo size is accompanied by an increase of free energy. On the other hand, if the size exceeds the critical size, further increase of embryo sizes leads to a reduction in free energy. Thus stable nuclei are generated.

3.1. Effect of nanoparticles on foam morphology

To obtain foam cells with a controlled structure and uniform distribution, a common practice is to add particles (nucleation agents) to reduce the nucleation free energy. Among them, the inorganic nucleation agents are most commonly used [7]. A fine dispersion of these nucleation agents can facilitate the formation of nucleation centers for a gaseous phase. Although the nucleation mechanism is still under investigation, it is generally known that the size, shape and distribution of the particles, as well as the surface treatment, can affect the nucleation efficiency. Nucleation in PS microcellular foaming using zinc stearate additives was investigated [138–140]. It was found that above the zinc stearate solubility limit, heterogeneous nucleation dominates and the nucleation rate increases with stearate concentration but is not affected by gas pressure. The presence of fillers was also shown to promote the accumulation of gas on the polymer–particle interface and creation of nucleation sites [141]. Furthermore, foams with finer fillers show a higher cell density at a high saturation pressure. Generally, the particles used in these studies are of micron size.

The amount and distribution of the nucleation agents are also important factors to determine the foam quality

[142]. The cell density is determined by the concentration of the foaming agent. A non-uniform distribution of the nucleation agents results in a foam that has more cells in the agent rich area and less cells in agent deficient areas, leading to a non-uniform cell size distribution in the foam product. Because the number and size of the bubbles are determined by the concentration of the foaming agent, the uniformity of the cell structure and the cell density are limited by the method used to mix the foaming agents and the polymer. In fact, it is difficult to obtain a uniform cell structure with a high cell density in the conventional foaming process.

Compared to conventional micron-sized filler particles used in the foaming processes, nanoparticles offer unique advantages for enhanced nucleation. The improved nucleation efficiency is reported in many studies for different polymer/nanoparticle systems at very low particle concentrations, e.g., PP/clay [110], PS/clay [64,65,109], Nylon/clay [124], PLA/clay [112,113], PC/clay [114], PU/clay [11,12], PVC/clay [100] and PS/CNFs and PS/CNTs [50,143]. The extremely fine dimensions and large surface area of nanoparticles provide much more intimate contact between the particles, polymer matrix, and gas. Furthermore, a significantly higher effective particle concentration can be achieved at a low nominal particle concentration. Both could lead to improved nucleation efficiency. The effect of particle concentration on the foam nucleation was investigated [100,108,110,113]. The cell density was found to increase linearly vs. clay concentration at low clay concentration, and starts to level off as clay concentration increases to 10% in some cases [108,113], while in other cases, an abrupt increase of cell density was observed as the clay concentration is increased [110].

The effect of clay nanoparticle dispersion on the foam cell morphology was studied in detail [59,64,65]. Both intercalated and exfoliated PS/clay nanocomposites were synthesized via in situ polymerization. The exfoliated nanocomposites yielded a much higher nucleation rate than the intercalated nanocomposites. This is attributed to the fact that even at the same nominal particle concentration, the effective particle concentration is higher once the particles are better dispersed. Consequently, more heterogeneous nucleation sites are available.

The effect of nanoparticles on cell size was also studied. It was found that in the presence of nanoparticles, the cell size is reduced. As more bubbles start to nucleate concurrently, there is a less amount of gas available for bubble growth, leading to a reduction of cell size. Moreover, the nanoparticles can significantly increase the melt viscosity. Strain induced hardening was observed under elongation as a result of the nanoclay alignment [144]. Both will hinder the cell growth and lead to a reduced cell size.

The surface chemistry of clay nanoparticles not only affects the particle dispersion but also has a tremendous effect on the nucleation efficiency in a polymer–clay–foaming agent system. MHAB modified nanoclay can covalently bond either styrene or MMA chains on the clay surface via in situ polymerization as shown in Schematic 1. The nature of the polymer tethered to the clay surface has a dramatic impact on the resulting foam morphology because of the interactions of CO_2 with the interfacial region between clay and polymer [64]. Here, surface polymerization of CO_2-philic PMMA produced exfoliated nanocomposites. The strong interactions between CO_2 and the surface-anchored PMMA also substantially reduced the nucleation free energy and enhanced the nucleation rate. Twentyfold increase in cell density was achieved via an addition of 2% clay in PS as shown in Fig. 4 [59]. Fig. 5 shows a comparison between several types of nanocomposite foams. The designation 20A is a composite produced by the physical mixing of a commercially available montmorillonite clay (Southern Clay) with polymer resulting in an intercalated structure. All MHABS composites are produced via in situ polymerization and have an exfoliated structure.

The parenthesis denotes in Fig. 5 is the monomer used for polymerization with MHABS. The in situ polymerized composite was then physically mixed with

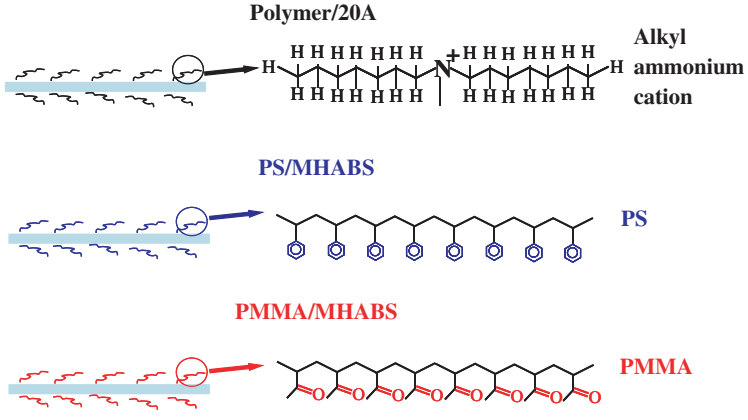

Schematic 1. Interfacial polymers on clay surface.

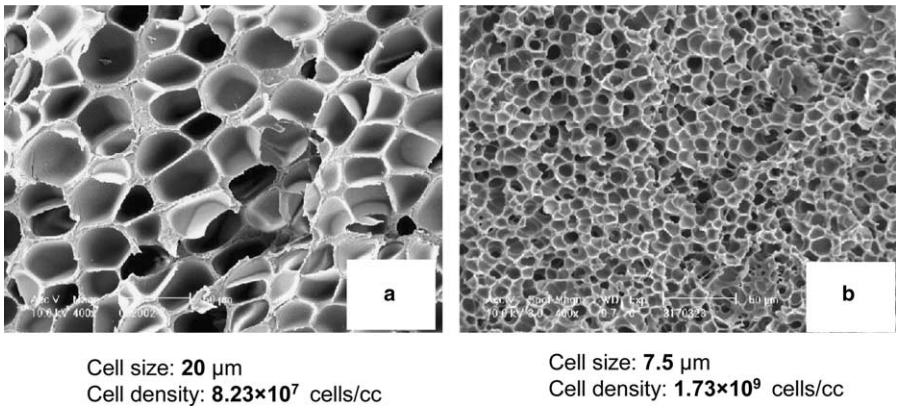

Fig. 4. Comparison of cell morphology of PS foams (a) pure PS (b) PS/2% MHABS nanocomposite with PMMA present on clay surface.

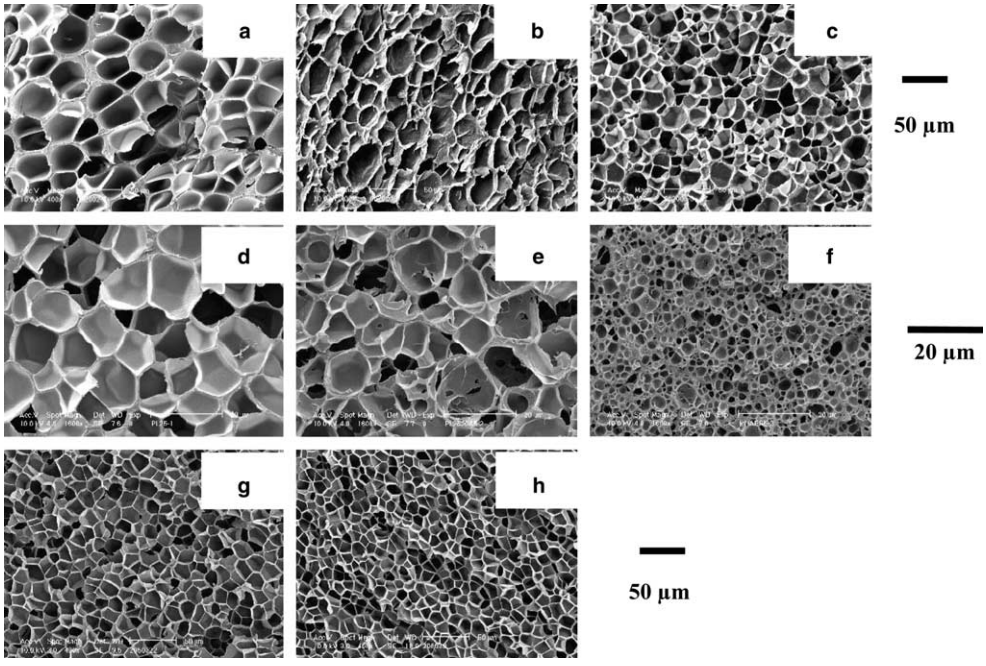

Fig. 5. SEM images of foams: (a) PS; (b) PS/5% 20A; (c)PS/5% MHABS; (d) PMMA; (e) PMMA/5% 20A; (f) PMMA/5% MHABS, (g) (PS/MHABS)/PMMA, (h) PS/(MHABS/PMMA).

a second polymer, e.g. (PS/MHABS)/PMMA denotes MHABS in situ polymerized with PS after which the excess PS was washed out and the composite compounded again with pure PMMA.

The difference in available nucleation sites is not responsible for the dramatic variation in cell density, as MHABS is well dispersed in both PS and PMMA matrices. The main difference between the copolymers tethered on the clay surface in PMMA/MHABS and that in PS/MHABS is that in PMMA/MHABS, the copolymer is essentially PMMA with a cationic ammonium head group bonded to the clay surface, whereas the copolymer in PS/MHABS is a PS polymer containing one methacrylic group. The former has a much higher affinity to CO_2 due to the interaction between CO_2 and the carbonyl groups in PMMA. More CO_2 is likely to be attracted to the surface to form nuclei. Additionally, a strong affinity between CO_2 and the carbonyl group of the tethered copolymers in PMMA/MHABS may reduce the gas-particle interfacial tension and consequently the contact angle. This would lead to the reduction in the work of nucleus formation and a large increase in nucleation rate.

This hypothesis is verified by two foams shown in Figs. 6(g) and (h). The (PS/MHABS)/PMMA has a cell size of 11.1 μm and a cell density of 6.25×10^8 cells/cm^3, whereas the PS/(MHABS/PMMA) has a smaller cell size (8.8 μm), and cell density almost two times higher (1.23×10^9 cells/cm^3). The clay remains exfoliated in the former whereas the latter possesses an intercalated structure due to collapse of the exfoliated structure after the extraction of free PMMA. Subsequent blending with PS only yielded

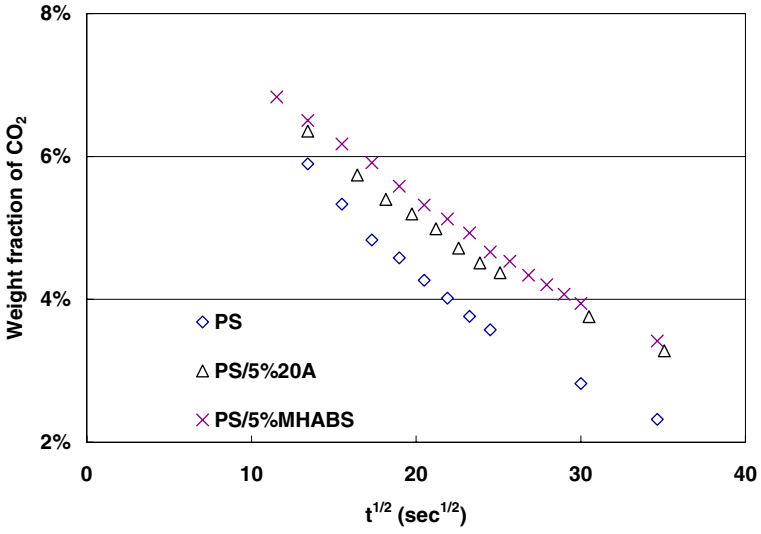

Fig. 6. CO_2 desorption from PS and PS nanocomposites at room temperature.

intercalated nanocomposites. Although PS/(MHABS/PMMA) has fewer nucleation sites (being intercalated), it yields a higher cell density. This increase can be attributed to the reduction of nucleation free energy as a result of the presence of PMMA at the polymer–clay–CO_2 interface. In PMMA/MHABS, the exfoliated structure ensures the highest number of available nucleation sites, and the interfacial PMMA at clay surface leads to the reduction of the nucleation free energy. A combination of these two factors results in the extremely high nucleation efficiency as observed in Fig. 5(f).

Fig. 6 shows CO_2 desorption curves of three samples, PS, PS/5% 20A, and PS/5% MHABS. After releasing the pressure in the high-pressure vessel, the samples remained unfoamed at low temperatures, and thus the dimensions of the samples remained unchanged. By extrapolating the desorption data back to time zero, the solubility of CO_2 in PS, PS/5% 20A, and PS/5% MHABS at 50 °C and 10 MPa was found to be 8.5, 8.5, and 8.8 wt%, respectively. Carbon dioxide exhibits a slightly higher solubility in the exfoliated PS nanocomposite. The diffusivity at room temperature was calculated based on the three desorption curves by assuming a one-dimensional diffusion since the sample thickness is much smaller than the other two dimensions. The results are 5×10^{-7}, 3×10^{-7}, and 3×10^{-7} cm^2/sec for PS, PS/5% 20A, and PS/5% MHABS respectively. Obviously, the addition of nanoclay can slow down the CO_2 diffusion out of the sample.

In addition to nanoclay, CNFs and CNTs have also been utilized to prepare PS nanocomposite foams [50,143]. In both cases, the incorporation of a small amount of nanoparticles leads to a microcellular cell structure, as shown in Fig. 7. Compared to the pure PS foam, the addition of 1 wt% of CNFs yields an increase of cell density by more than two orders, while the cell size decreases from 20 to 2.64 μm. CNTs also exhibit a good nucleation effect. Although with poor particle dispersion, the resultant PS foam with 0.1 wt% CNTs still displays a high cell density and a small cell size (Fig. 7(c)). The average cell density is 1.44×10^9 cells/cm^3 and the average cell size is 7.11 μm.

A similar effect of nanoclay on reducing the cell size and increasing the cell density has been observed in the thermoset PU nanocomposite foam system at 5% clay content [12]. The efficiency of nanoclay on size reduction in this system, however, was not as strong as that in thermoplastics foams. Clay orientation and dispersion is somewhat affected by the foaming process.

3.2. Bubble nucleation in nanocomposites

The classical nucleation theory is the approach currently used to describe bubble nucleation in polymer foams, although its prediction of the nucleation rate can easily be off by several orders of magnitude. Within the polymer foaming community, the discrepancy between the classical theory and experiments is sometimes attributed to the intervening heterogeneous nucleation [145] or has led to modifications of the classical theory by incorporating certain aspects specific to the polymer foaming process [138–140,146–148].

The essential content of the classical theory is as follows [149]. The steady state nucleation rate, N_0, is given by:

$$N_0 = C_0 f_0 \exp\left(-\frac{\Delta G_{\text{crit}}}{k_B T}\right), \tag{1}$$

where ΔG_{crit}, k_B, and T denote, respectively, the free energy of critical nucleus formation, the Boltzmann factor, and the absolute temperature. C_0 is the number of gas molecules dissolved per unit volume of the primary phase, and f_0 is a kinetic preexponential factor that is

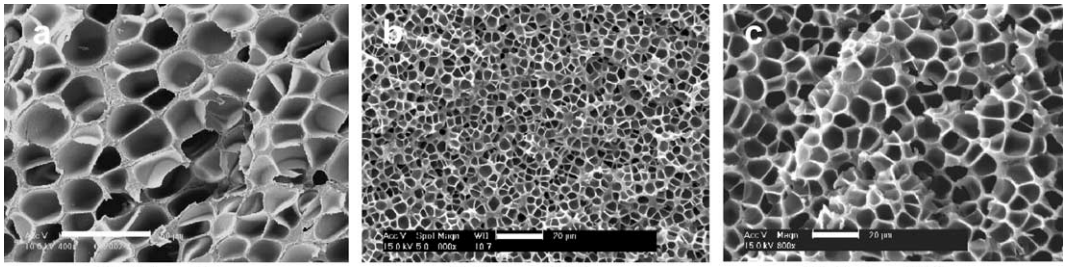

Fig. 7. Cell morphologies of: (a) PS foam (scale bar 50 μm) (b) PS/1% CNFs nanocomposite foam (scale bar 20 μm) and (c) PS/0.1% CNTs nanocomposite foam (scale bar 20 μm).

believed to be weakly dependent upon temperature [150].

Since ΔG_{crit} appears in the exponent, ΔG_{crit} has a strong impact on the foam quality [151,152]. The classical theory draws from the following formally exact expression for ΔG_{crit} [153]:

$$\Delta G_{crit} = \frac{16\pi\sigma^3}{3\Delta P^2}, \tag{2}$$

where ΔP denotes the difference between two pressures, one pertaining to the nucleating phase if it existed in bulk at the same temperature and chemical potential as the metastable phase, and the other to the metastable phase (created by imposing a thermodynamic instability on a stable polymer/gas solution). If the polymer is fully saturated with CO_2 and the partial molar volume of CO_2 in the polymer is zero, ΔP can be taken as the difference between pressure inside and outside the nucleating bubble or as the pressure drop required to induce nucleation ($P_{initial}$–P_{final}) [10,138]. However, our recent study showed that these assumptions may induce an overestimation of the energy requirement. Another difficulty in applying Eq. (2) lies in the fact that σdepends on the size of the critical bubble (nucleus) and usually is inaccessible by experiments. Thus, the classical nucleation theory introduces an approximation of replacing $\sigma$by the surface tension of the macroscopic bubble/polymer interface, which can be measured.

Nanoparticles undoubtedly serve as heterogeneous nucleation agents and their effect on cell density has been qualitatively described by the classical nucleation theory [138–140]. In the case of heterogeneous nucleation, the nucleation rate is expressed as

$$N_1 = C_1 f_1 \exp\left(-\frac{\Delta G^{het}_{crit}}{k_B T}\right), \tag{3}$$

where f_1 is the frequency factor of gas molecules joining the nucleus and C_1 is the concentration of heterogeneous nucleation sites. The work of forming a critical nucleus in a heterogeneous system, ΔG^{het}_{crit} is considered proportional to the work in a homogeneous system (Eq. (2)) by a factor dependent on the contact angle θ between the gas and polymer and particle surface

$$\Delta G^{het}_{crit} = \frac{16\pi\sigma^3}{3(P^G - P^L)^2} S(\theta), \tag{4}$$

$$S(\theta) = (1/4)(2+\cos\theta)(1-\cos\theta)^2. \tag{5}$$

In addition to the contact angle, the surface curvature of particles also plays an important role in the critical nucleation energy [154]. The dependency of ΔG^{het}_{crit} on both the surface curvature and the contact angle can be described by

$$\Delta G^{het}_{crit} = \frac{16\pi\sigma^3}{3(P^G - P^L)^2} \frac{f(m,w)}{2}. \tag{6}$$

Here, $f(m,w)$ is the energy reduction factor, which is a function of θ and the relative curvature (w) of the nucleant surface (radius R) to the critical radius (r_{crit}) of the nucleated phase

$$f(m,w) = 1 + \left(\frac{1-mw}{g}\right)^3 + w^3\left[2 - 3\left(\frac{w-m}{g}\right) + \left(\frac{w-m}{g}\right)^3\right] + 3mw^2\left(\frac{w-m}{g} - 1\right), \tag{7}$$

$$m = \cos\theta, \tag{8}$$

$$w = R/r_{crit}, \tag{9}$$

$$r_{crit} = \frac{2\sigma}{P_G - P_L}, \tag{10}$$

$$g = (1 + w^2 - 2mw)^{\frac{1}{2}}. \tag{11}$$

In heterogeneous nucleation, the highest nucleation efficiency can only be achieved when the nucleation on the nucleant surface is energetically favored (relative to its homogeneous counterpart) and the nucleant is dispersed in the polymer matrix. In most cases, the observed cell density is much lower than the potential nucleant density, implying that either the nucleants are not energetically effective, or their effects have been compromised due to poor dispersion. The nucleation efficiencies of CNFs, CNTs and exfoliated nanoclay were compared in a recent study [63].

The potential nucleant density in a heterogeneous nucleation system can be estimated by Eq. (12) [155]:

$$\frac{\text{Nucleants}}{\text{cm}^3} = \frac{w}{\rho_P}\frac{\rho_{blend}}{V_P}, \quad (12)$$

where w is the weight fraction of the particle in the composite, ρ_P is the density of the particle, ρ_{blend} is the density of the polymer blend, and V_P is the volume of the individual particle. In the case of CNFs, the potential nucleant density of the PS composite containing 1 wt% CNFs is $1.41 \times 10^{12}/\text{cm}^3$ according to Eq. (12). Experimentally, the cell density of the foam with the same fiber content is 2.78×10^{10} cells/cm^3 (shown in Fig. 7(b)). The proximity of these two values indicates that most of the fibers served well as nucleants in the PS foaming. The nucleation efficiency, defined by the ratio of the measured cell density to the potential nucleant density, is 1.97% for CNFs. Similar calculations were conducted for PS/MHABS and PS/CNTs foams and the results are listed in Table 2. For both clay and CNTs systems, the potential nucleant densities are much higher than the final cell densities, leading to nucleation efficiencies that are orders of magnitude lower than that of CNFs.

Fig. 8 illustrates how the reduction of critical energy is affected by the nucleants, in terms of surface property (contact angle) and particle geometry (nucleant curvature). Qualitatively, a small contact angle and a large surface curvature offer a higher reduction of critical energy, and consequently an increased nucleation rate [154].

Under the foaming conditions ($T = 120$ °C, $P = 13.8$ MPa), σ was calculated to be ~16.43 mJ/m^2 from the known PS-CO_2 surface tension value from the literature [156,157], r_{crit} is 2.38 nm from Eq. (10). Thus the relative radius w is around 21 for individual CNF. With a typical contact angle of 20° [138], Eq. (7) yields a reduction factor f of 0.006, indicating that the energy required for the bubble nucleation (ΔG^{het}_{crit}) on the surfaces of CNFs is only 0.003 ($f/2$) of that in the homogeneous case. In addition, since a complete dispersion of CNFs in the PS matrix was achieved (as shown in Fig. 3), the actual nucleant density is close to the calculated one. The combination of the low energy barrier and the high nucleant density results in a high nucleation rate and ultimately a high cell density.

In the PS/CNTs system, if the CNTs are completely dispersed, the relative radius w is only 0.2 considering that the radius of an individual tube is 0.5 nm. In that case, f is 1.8 and the nucleation energy on any single tube surface would approach the homogeneous limit, completely diminishing the benefit of heterogeneous nucleation. However, experimentally, most CNTs were observed as spherical agglomerates with an average radius of approximately several dozen nanometers. These agglomerates with much larger radii can serve as lower nucleation energy sites, but the actual nucleant density is much lower than the theoretical value owing to poor dispersion, leading to the compromised nucleation efficiency.

In the PS/MHABS system, the relatively low nucleation efficiency can be explained first by incomplete par-

Table 2
Comparison of potential nucleus density and actual cell density

Nanoparticle	wt%	Dispersion[a]	Potential nucleant density[b] (#/cm^3)	Measured cell density (#/cm^3)	Efficiency (%)
CNF	1	Complete	1.41×10^{12}	2.78×10^{10}	1.97
CNT	0.1	Aggregates	1.59×10^{15}	1.44×10^{9}	9.06×10^{-5}
MHABS	5	Exfoliated	5.45×10^{13}	4.02×10^{8}	7.37×10^{-4}

[a] Actual particle dispersion observed by TEM images.
[b] Calculated (Eq. (1)) with the assumption of complete particle dispersion [63].

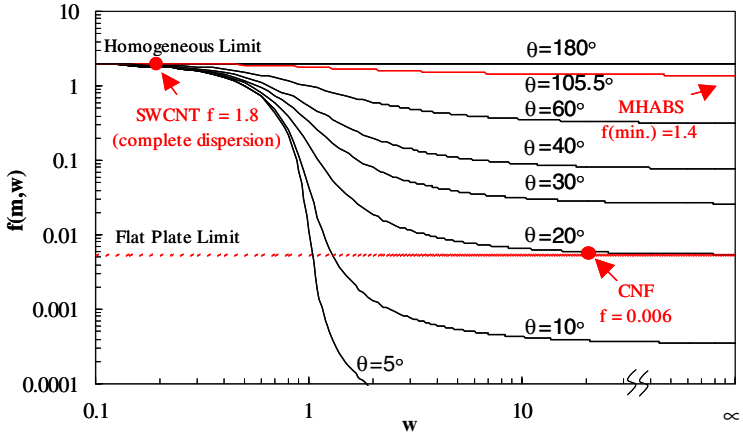

Fig. 8. Reduction of critical nucleation energy by function $f(m, w)$.

ticle dispersion. Although exfoliated, stacks of multiple layers are still observable in the polymer domain [65]. A rough estimation from the TEM image of PS/5% MHANBS indicates an average stack thickness on the orders of tens of nanometers [65]. Therefore, the actual nucleant density in the PS/5% MHABS system would be reduced by one order from the value shown in Table 2, i.e., from 5.45×10^{13} to $5.45 \times 10^{12}/cm^3$. This value, however, is still much higher than the measured cell density ($4.02 \times 10^8/cm^3$), suggesting that there must be other reasons accounting for the low nucleation efficiency. On the clay surface, the nucleation energy should approach the flat plate limit ($R \to \infty$) due to the layered structure of the nanoclay. The modified clay surface is more compatible with the PS matrix, and thus the interfacial tension of the PS melt and the clay is expected to be lower than that of PS and CNFs. Consequently, the contact angle θ would be higher. This would lead to a significant increase of f, or much less reduction of nucleation free energy. The equilibrium interfacial tension data in the literature [158] show the lower limit of θ to be 105.5° [63]. This leads to a minimum reduction factor f of 1.4 and a reduction of nucleation free energy by 30%. Although the PS/5% MHABS system has a much higher number of potential nucleants than both the PS/1% CNFs and the PS/0.1% CNTs systems, its nucleation efficiency is greatly compromised by the relative ineffectiveness of the energy reduction [138–140].

3.3. Effect of nanoparticles on foam properties

The high aspect ratio and large surface area of nanoparticles offer the potential for high reinforcing efficiency, good barrier properties, and improved dimensional and thermal stability. The nanometer dimension is especially beneficial for reinforcing foam materials, considering the thickness of cell walls is in the micron and submicron regime. It is therefore ideal to use nanoparticles to reinforce microstructures in order to achieve macroscale property improvement of the final products.

Polymer nanocomposite foams exhibit substantially improved properties compared to their neat polymer foam counterparts. Blown by three parts by weight of CO_2, the PVC/3% Cloisite 30B nanocomposite foam shows 17.9% increase of tensile strength, 25.9% increase of bending strength and 250% increase of the elongation ratio compared to the pristine PVC foam [100]. The tensile modulus of PS/clay nanocomposite foams has been measured and compared to pure PS foam and PS/talc microcomposite foams. As shown in Fig. 9, the nanocomposite foams exhibit a higher reduced modulus (i.e., tensile modulus divided by the density of the sample), although it is still lower than that of non-foamed pure PS. Among the three foam samples, PS/talc, PS/5 wt% 20A, and PS/5 wt% MHABS, the densities are close while the exfoliated nanocomposite foam has the highest reduced modulus. Compared to the non-foamed PS sample, the exfoliated nanocomposite foam sample has about 31% weight reduction with a sacrifice in the reduced modulus of about 19% from 2.6 to 2.1 GPa/g/cm^3. In comparison, the PS/talc foam has about 29% weight reduction and a decrease of 43% in reduced modulus [65].

The tensile properties of extruded PS/CNFs nanocomposite foams have been investigated as well [50]. As shown in Fig. 10, all the foams exhibit a similar foam

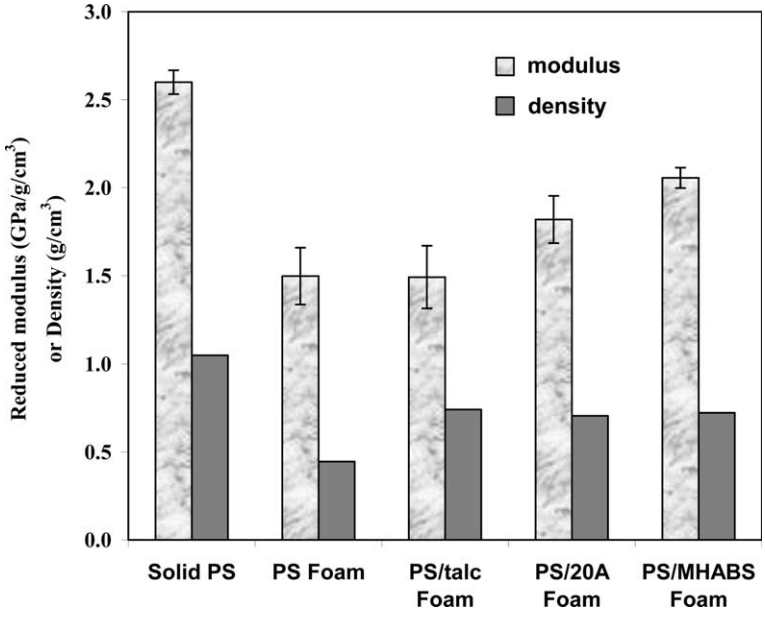

Fig. 9. Tensile modulus of PS/5% clay nanocomposite foams.

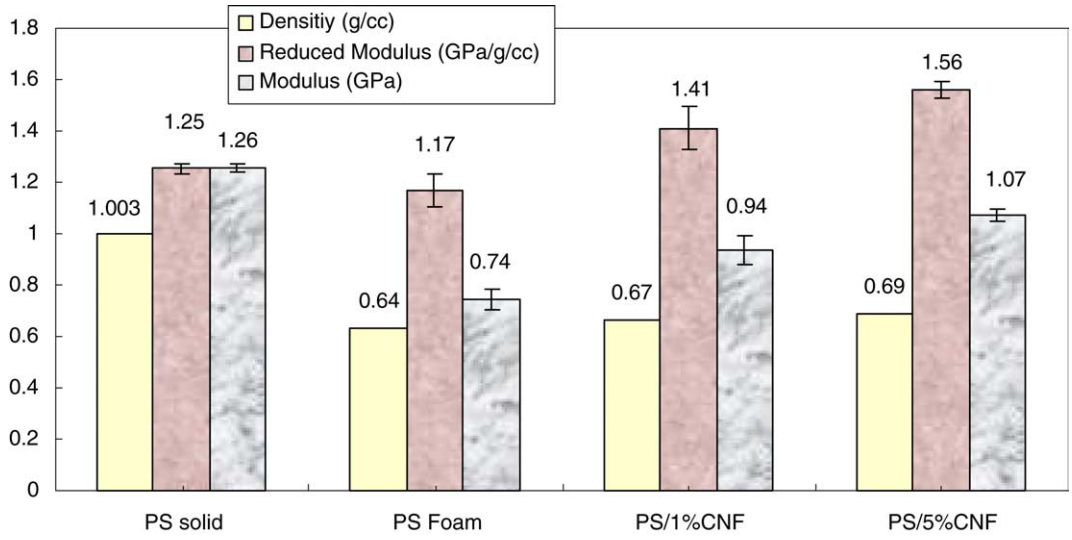

Fig. 10. Tensile modulus of extruded PS and PS/CNF nanocomposite foams.

density of 0.6–0.7 g/cm^3, indicating a similar weight reduction compared to the bulk PS. For neat PS foam, a weight reduction of 37% sacrifices the tensile modulus by 40% (1.26–0.74 GPa). In the presence of 1 wt% CNFs, the tensile modulus increases by 28% (0.74–0.94 GPa). Once the fiber content is increased to 5 wt%, the tensile modulus further increases to 1.07 GPa, which is comparable to that of the bulk PS (1.26 GPa). In order to normalize the impact of the foam density on the mechanical properties, reduced modulus was used to compare these samples. Due to the relatively lower densities, the reduced modulus of PS/CNFs foams is much higher than that of the bulk PS.

Using the batch foaming process, neat PS and PS/CNFs foams were generated with suitable dimensions for the tests of compressive properties. As shown in Fig. 11, the density of PS/CNFs foams falls in the range of 0.4–0.5 g/cm^3. In the presence of CNFs (both 1% and 5%), PS foams show even a higher compressive modulus than that of the PS solid. For example, PS foam containing 5% CNFs exhibits a 12.4% increase in the modulus and a 136% increase in the reduced modulus over the PS solid. This result indicates that the integration of

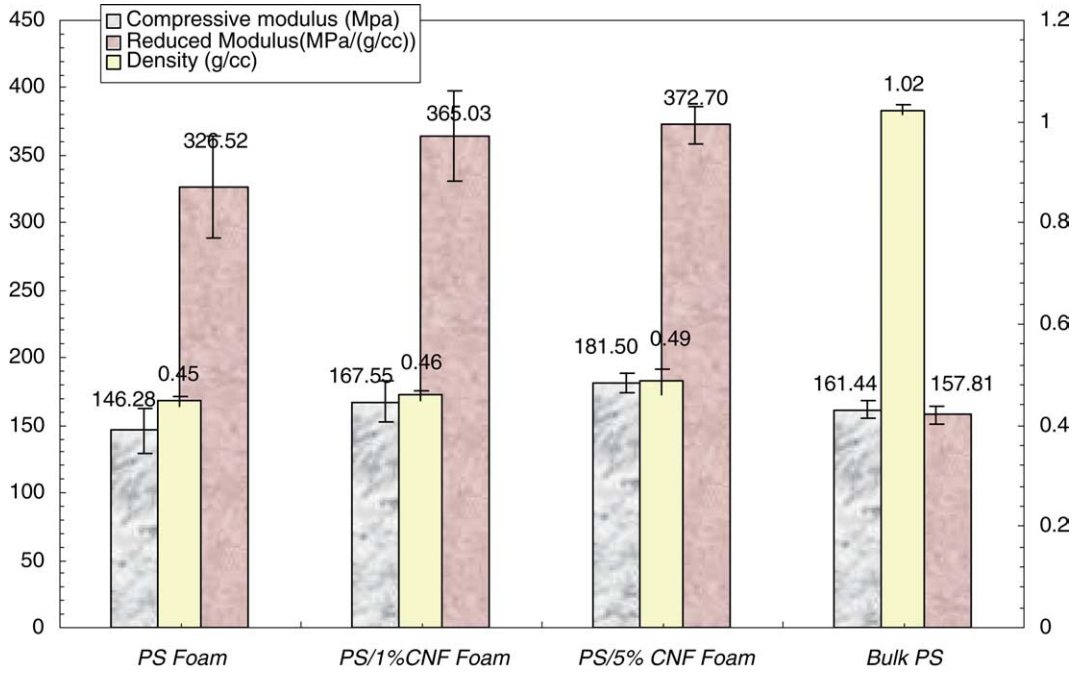

Fig. 11. Compressive modulus of PS and PS/CNF nanocomposite foams, synthesized by the batch foaming process (CO_2, 80 °C, 13.8 MPa).

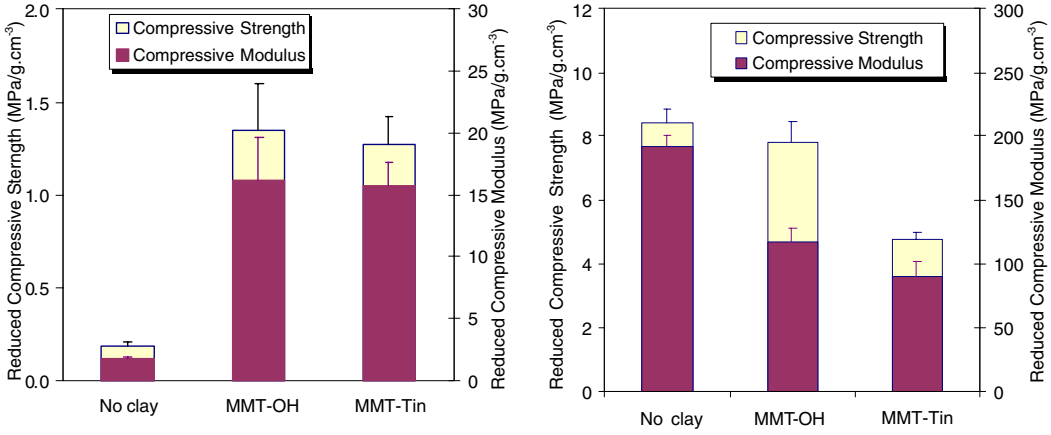

Fig. 12. Compressive properties of PU/5% clay nanocomposite foams, (a) polyol-180 (b) polyol-100.

CNFs into the PS foams have a great potential to bridge the gap between the lightweight and high strength requirements. On one hand, CNFs can effectively induce the nucleation of a large amount of bubbles, which ultimately provides a comparable weight reduction to the neat PS foams. On the other hand, the strength deterioration resulted from the inclusion of cells can be compensated by the reinforcement of cell walls/junctions by CNFs.

The fire retardance properties of nanocomposite foams have been demonstrated by Han et al. [65]. After burning, the PS nanocomposite foams formed char and maintained structural integrity, while the pure foams quickly melted and dripped, causing fire spreading. Char also forms for PVC nanocomposite foams [100]. The effects of nanoparticles on mechanical properties of thermoset PU/clay nanocomposite foam were also investigated [12]. Two types of nanoclay bearing different functional groups were used to prepare PU nanocomposite foam. Montomorrilonite–OH (MMT-OH) has hydroxyl groups on clay surface and MMT-Tin has catalytic organotin for polyurethane reaction. In the case of semi-flexible/semi-rigid foams (polyol with equivalent weight of 180, polyol-180), a several fold increase in both compressive strength and modulus were observed, again demonstrating high reinforcement efficiency of nanoparticles. However, for the rigid foam system (polyol with equivalent weight of 100, polyol-100), the presence of clay nanoparticles can interfere with the hydrogen bond formation and network structure in the matrix, leading to reduced mechanical properties (i.e. compressive strength and modulus divided by the density of the foam sample) as shown in Fig. 12. It is well known that H-bond formation among urethane groups greatly contributes to the strength and modulus of PUs. For the organoclays used in this study, the PU molecules can be grafted onto the clay surface through the reaction between the –NCO groups and the –OH groups on the clay. The tethered clay may interfere with the H-bond formation in PU as shown in Schematic 2, causing a negative effect on the properties of PU nanocomposite foams. Furthermore, the involvement of organoclays in the reaction could also affect the network structure formation of PU. For PU foams prepared by poly-100, the urethane content is 0.87 mol/100 g, while the urethane content is only 0.65 mol/100 g for the foams prepared by polyol-180. The overall performance of PU nanocomposite foams depends on the competition between the positive effects of clay on polymer reinforcement and foam morphology, and the negative effects on H-bond formation and network structure. The positive effects are stronger for the less rigid polyol-180 foams, while the negative effects dominate for the more rigid polyol-100 foams. The same effect was observed for the rigid PU/nano-silica nanocomposite foam, in which the compressive strength decreases with the higher usage of nano-silica [136]. Nanoclay has also been demonstrated to improve the thermal insulation and aging properties of PU foam (indicated by *k*-factors in Btu.in/ft^2.h.F). The foam with 10% nanoclay gave lower initial and aged k-factors, indicating better thermal insulation [130].

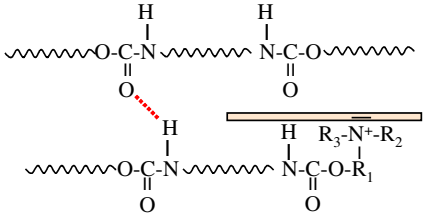

Schematic 2. The interference of grafted clay on H-bond formation in polyurethane.

4. Conclusions and future trends

Due to the high nucleation efficiency, nanoparticles provide a powerful way to increase cell density and

reduce cell size. This is particularly beneficial for the production of microcellular foams. Microcellular foams have been considered as a lightweight and high strength material for structural applications. However, the narrow operation window and less than desirable cell morphology has limited the applications of this technology. Adding nanoparticles is possible to resolve this difficulty and may greatly enhance the industrial applications of microcellular foam.

Mass production of polymer nanocomposites and nanocomposite foams depends on reliable and affordable synthetic and processing methods. The literature is full of novel nanocomposite materials. But in order to move these materials into commercial products, several challenges must be overcome. There must be robust techniques to prepare exfoliated nanocomposites with required mechanical properties in large quantity and low cost. For foam products, various desirable cell morphologies (e.g., small vs. large cells, open vs. closed cells) must be attainable through the successful control of nucleation and growth of bubbles.

It has been found that the surfactant, introduced onto the clay surface to achieve good compatibility between the inorganic clay and the organic polymer or monomer for good clay exfoliation, is a fire hazard material. Natural clay without surface modification, however, can only disperse well in water-soluble polymers. Using water as a nanoclay carrier may achieve surfactant-free nanocomposites with good clay dispersion in hydrophobic polymers. We are currently developing a new method for nanocomposite synthesis by inverse emulsion/suspension polymerization. This technique has been used extensively to prepare water expandable polystyrene (WEPS) [159–165].

Open cell polymer foams are one of the most commonly used scaffolds for tissue engineering. Nanoparticles may be helpful in generating open cell foams under external fields such as ultrasonic fields, because nanoparticles may behave like a stress concentrator. This may led to a new mass production technology for tissue engineering scaffolds. The high surface area and rich surface chemistry make nanoparticles potentially useful as carriers for desired biofunctionalities (e.g., adhesion sites and signaling molecules).

References

[1] Giannelis EP. Polymer layered silicate nanocomposites. Adv Mater (Weinheim, Germany) 1996;8(1):29.

[2] Alexandre M, Dubois P. Polymer-layered silicate nanocomposites: preparation, properties and uses of a new class of materials. Mater Sci Eng, R: Reports 2000;R28(1–2):1.

[3] Vaia RA, Giannelis EP. Polymer nanocomposites: Status and opportunities. MRS Bull 2001;26(5):394.

[4] Hammel E, Tang X, Trampert M, Schmitt T, Mauthner K, Eder A, et al. Carbon nanofibers for composite applications. Carbon 2004;42(5–6):1153.

[5] Zhu J, Kim J, Peng H, Margrave JL, Khabashesku VN, Barrera EV. Improving the dispersion and integration of single-walled carbon nanotubes in epoxy composites through functionalization. Nano Lett 2003;3(8):1107.

[6] Safadi B, Andrews R, Grulke EA. Multiwalled carbon nanotube polymer composites: synthesis and characterization of thin films. J Appl Polym Sci 2002;84(14):2660.

[7] Klempner D, Frisch KC, editors. Handbook of polymeric foams and foam technology. New York: Oxford University Press; 1991.

[8] Mikos AG, Temenoff JS. Formation of highly porous biodegradable scaffolds for tissue engineering. J Biotechnol 2000;3(2):1.

[9] www.azom.com/details.asp?articleID=1557; 2001.

[10] Lee S-T. Foam extrusion: principles and practice. Lancaster, PA: Technomic Publishing Company Inc.; 2000.

[11] Cao X, Lee LJ, Widya T, Macosko C. Structure and properties of polyurethane/clay nanocomposites and foams. 62nd ed. Annual technical conference, vol. 2. Society of Plastics Engineers; 2004. p. 1896.

[12] Cao X, Lee LJ, Widya T, Macosko C. Polyurethane/clay nanocomposites foams: processing, structure and properties. Polymer 2005;46(3):775.

[13] Theng BKG. The chemistry of clay-organic reactions. New York: Wiley; 1974.

[14] Zhu J, Kim J, Peng H, Margrave JL, Khabashesku VN, Barrera EV. Nano Lett 2003;3:1107.

[15] Liao K, Li S. Appl Phys Lett 2001;79:4225.

[16] Qian D, Dickey EC, Andrews R, Rantell T. Appl Phys Lett 2000;76:2868.

[17] Sandler J, Shaffer MSP, Prasse T, Bauhofer W, Schulte K, Windle AH. Polymer 1999;40:5967.

[18] Gong X, Liu J, Baskaran S, Voise RD, Young JS. Chem Mater 2000;12:1049.

[19] Hill DE, Lin Y, Rao AM, Allard LF, Sun Y-P. Macromolecules 2002;35:9466.

[20] Safadi B, Andrews R, Grulke EA. J Appl Poly Sci 2002;84:2660.

[21] Mitchell CA, Bahr JL, Arepalli S, Tour JM, Krishnamoorti R. Macromolecules 2002;35:8825.

[22] Vaia RA, Sauer BB, Tse OK, Giannelis EP. Relaxations of confined chains in polymer nanocomposites: glass transition properties of poly(ethylene oxide) intercalated in montmorillonite. J Poly Sci: Part B: Polym Phys 1997;35(1):59.

[23] Ogata N, Kawakage S, Ogihara T. Poly(vinyl alcohol)-clay and poly(ethylene oxide)-clay blends prepared using water as solvent. J Appl Polym Sci 1997;66:573.

[24] Billingham J, Breen C, Yarwood J. Vibrat Spectros 1997;14:19.

[25] Kymakis E, Alexandou I, Amaratunga GAJ. Synth Mater 2002:59.

[26] Liu L, Qi Z, Zhu X. Studies on nylon 6/clay nanocomposites by melt-intercalation process. J Appl Polym Sci 1999;71:1133.

[27] Lincoln DM, Vaia RA, Wang ZG, Hsiao BS. Secondary structure and elevated temperature crystallite morphology of nylon-6/layered silicate nanocomposites. Polymer 2001;42:1621.

[28] Dennis HR, Hunter DL, Chang D, Kim S, White JL, Cho JW, et al. Effect of melt processing conditions on the extent of exfoliation in organoclay-based nanocomposites. Polymer 2001;42(23):9513.

[29] Cho JW, Paul DR. Nylon 6 nanocomposites by melt compounding. Polymer 2001;42:1083.

[30] Fornes TD, Yoon PJ, Keskkula H, Paul DR. Nylon 6 nanocomposites: the effect of matrix molecular weight. Polymer 2001;42(25):09929.

[31] Vaia R. A polymer melt intercalation in mica-type layered silicates. Cornell University, Department of Materials Science and Engineering; 1995.

[32] Vaia RA, Giannelis EP. Polymer Melt Intercalation in Organically-Modified Layered Silicates: Model Predictions and Experiment. Macromolecules 1997;30(25):8000.
[33] Vaia RA, Jandt KD, Kramer EJ, Giannelis EP. Microstructural evolution of melt intercalated polymer-organically modified layered silicates nanocomposites. Chem Mater 1996;8(11): 2628.
[34] Manias E, Chen H, Krishanmoorti R, Genzer J, Kramer EJ, Giannelis EP. Intercalation kinetics of long polymers in 2 nm confinements. Macromolecules 2000;22:7955.
[35] Svoboda P, Zeng C, Wang H, Lee LJ, Tomasko DL. Morphology and mechanical properties of polypropylene/organoclay nanocomposites. J Appl Polym Sci 2002;85:1562.
[36] Kato M, Usuki A, Okada A. Synthesis of polypropylene oligmer-clay intercalation compounds. Journal of Appled Polymer Science 1997;66:1781.
[37] Kawasumi M, Hasegawa N, Kato M, Usuki A, Okada A. Macromolecules 1997;30:6333.
[38] Hasegawa N, Kawasumi M, Kato M, Usuki A, Okada A. Preparation and mechanical properties of polypropylene-clay hybrid using a maleic anhydride-modified polypropylene oligomer. J Appl Polym Sci 1998;67:87.
[39] Gilman JW, Jackson CL, Morgan AB, Harris Jr R, Manias E, Giannelis EP, et al. Flammability properties of polymer-layered silicate nanocomposites. Polypropylene and polystyrene nanocomposites. Chem Mater 2000;12(7):1866.
[40] Nam PH, Maiti P, Okamoto M, Kotaka T, Hasegawa N, Usuki A. A hierarchical structure and properties of intercalated polypropylene/clay nanocomposites. Polymer 2001;42(23):9633.
[41] Galgali G, Ramesh C, Lele A. A rheological study on the kinetics of hybrid formation in polypropylene nanocomposites. Macromolecules 2001;34(4):852.
[42] Reichert P, Nitz H, Klinke S, Brandsch R, Thomann R, Mulhaupt R. Poly(propylene)/organoclay nanocomposite formation: influence of compatibilizer functionality and organoclay modification. Macromol Mater Eng 2000;275:8.
[43] Vaia RA, Giannelis EP. Lattice model of polymer melt intercalation in organically-modified layered silicates. Macromolecules 1997;30(25):7990.
[44] Zhulina E, Singh C, Balazs AC. Attraction between surfaces in a polymer melt containing telechelic chains: guidlines for controlling the surface separation in intercalated polymer–clay composites. Langmuir 1999;15(11):3935.
[45] Ginzburg VV, Balazs AC. Predicting the phase behavior of polymer-clay nanocomposites: the role of end-functionalized chains, ACS Symposium Series. Polymer Nanocomposites 2002;804:57.
[46] Ginzburg VV, Balazs AC. Calculating phase diagrams for nanocomposites: the effect of adding end-functionalized chains to polymer/clay mixtures. Adv Mater (Weinheim, Germany) 2000;12(23):1805.
[47] Mitchell CA, Bahr JL, Arepalli ea S. Macromolecules 2002;35(23):8825.
[48] Ma H, Zeng J, Realff ea ML. Compos Sci Technol 2003;63:1617.
[49] Ravich D, Lips D. Compos Sci Technol 2002;62:1105.
[50] Shen J, Han X, Lee LJ. Nucleation and reinforcement of carbon nanofibers on polystyrene nanocomposite foam. 63rd ed. Annual technical conference. Society of Plastics Engineers; 2005. p. 1896. ASAP.
[51] Usuki A, Kojima Y, Kawasumi M, Okada A, Fukushima Y, Kurauchi T, et al. Synthesis of nylon 6-clay hybrid. J Mater Res 1993;8(5):1179.
[52] Messersmith PB, Giannelis EP. Synthesis and barrier properties of poly(.epsilon.-caprolactone)-layered silicate nanocomposites. J Polym Sci, Part A: Polym Chem 1995;33(7):1047.
[53] Pinnavaia TJ, Lan T, Wang Z, Shi H, Kaviratna PD. Clay-reinforced epoxy nanocomposites: synthesis, properties, and mechanism of formation. ACS Symposium Series 1996;622:250 (Nanotechnology).
[54] Huang X, Lewis S, Brittain WJ, Vaia RA. Synthesis of polycarbonate-layered silicate nanocomposites via cyclic oligomers. Macromolecules 2000;33(6):2000.
[55] Weimer MW, Chen H, Giannelis EP, Sogah DY. Direct synthesis of dispersed nanocomposites by in situ living free radical polymerization using a silicate-anchored initiator. J Am Chem Soc 1999;121(7):1615.
[56] Huang X, Brittain WJ. Synthesis and characterization of PMMA nanocomposites by suspension and emulsion polymerization. Macromolecules 2001;34(10):3255.
[57] Fu X, Qutubuddin S. Synthesis of polystyrene-clay nanocomposites. Mater Lett 2000;42(1-2):12.
[58] Zeng C, Lee LJ. Poly(methyl methacrylate) and polystyrene/clay nanocomposites prepared by in situ polymerization. Macromolecules 2001;34(12):4098.
[59] Zeng C. Polymer nanocomposites: synthesis, structure and processing, The Ohio State University, Chemical Engineering; 2003.
[60] Ying Z, Du J, Bai S, et al. Int J Nanosci 2002;1(5–6):425.
[61] Velasco C, Martinez AL, Fisher FT, et al. Chem Mater 2003;15:4470.
[62] Gong X, Liu J, Baskaran S, et al. Chem Mater 2000;12(4):1049.
[63] Shen J, Zeng C, Lee LJ. Synthesis of polystyrene-carbon nanofibers nanocomposite foams. Polymer 2005;46(14):5218.
[64] Zeng C, Han X, Lee LJ, Koelling KW, Tomasko DL. Polymer–clay nanocomposite foams prepared using carbon dioxide. Adv Mater (Weinheim, Germany) 2003;15(20):1743.
[65] Han X, Zeng C, Lee LJ, Koelling KW, Tomasko DL. Extrusion of polystyrene nanocomposite foams with supercritical CO2. Polym Eng Sci 2003;43(6):1261.
[66] Lee DC, Jang LW. J Appl Polym Sci 1996;61:1117.
[67] Noh MW, Lee DC. Polym Bull (Berlin) 1999;42:619.
[68] Biasci L, Alietto M, Ruggeri G, Ciardelli F. Polymer 1994;35:3296.
[69] Okamoto M, Morita S, Taguchi H, Kim YH, Kotaka T, Tateyama H. Polymer 2000;41:3887.
[70] Doh JG, Cho I. Polym Bull (Berlin) 1998;41:511.
[71] Bandyopadhyay S, Giannelis EP, Hsieh AJ. Polym Mater Sci Eng 2000;82:208.
[72] Aguilar-Solis C, Xu Y, Brittain WJ. PVC nanocomposites via emulsion and suspension polymerization, Polymer Preprints (American Chemical Society, Division of Polymer Chemistry), 43(2); 2002. p. 1019.
[73] Gong F, Feng M, Zhao C, Zhang S, Yang M. Thermal properties of poly(vinyl chloride)/montmorillonite nanocomposites. Polym Degrad Stability 2004;84(2):289.
[74] Gong FL, Zhao CG, Feng M, Qin HL, Yang MS. Synthesis and characterization of PVC/montmorillonite nanocomposite. J Mater Sci 2004;39(1):293.
[75] Hu H-Y, Pan M-W, Li X-C, Shi X-D, Zhang L-C. Studies on preparation and properties of PVC/organoclay nanocomposite. Gaofenzi Cailiao Kexue Yu Gongcheng 2004;20(5):162.
[76] Hu H, Pan M, Li X, Shi X, Zhang L. Preparation and characterization of poly(vinyl chloride)/organoclay nanocomposites by in situ intercalation. Polym Int 2004;53(2):225.
[77] Liang Z-M, Wan C-Y, Zhang Y, Wei P, Yin J. PVC/montmorillonite nanocomposites based on a thermally stable, rigid-rod aromatic amine modifier. J Appl Polym Sci 2004;92(1):567.
[78] Pan M, Shi X, Li X, Hu H, Zhang L. Morphology and properties of PVC/clay nanocomposites via in situ emulsion polymerization. J Appl Polym Sci 2004;94(1):277.
[79] Shi X, Pan M, Li X, Zhang L, Ding H. Studies on the morphology and properties of PVC/Na+-MMT nanocomposites prepared by in situ emulsion polymerization. Gaofenzi Xuebao 2004:149.

[80] Wan C, Qiao X, Zhang Y, Zhang Y. Methods for preparing a polyvinyl chloride/layered silicate nanocomposite. Faming Zhuanli Shenqing Gongkai Shuomingshu, Cn, 1400228; 2003.
[81] Wang D, Parlow D, Yao Q, Wilkie CA. PVC/clay nanocomposites: preparation, thermal and mechanical properties. J Vinyl Additive Technol 2001;7(4):203.
[82] Wu D, Wang X, Jin R. Study on toughness and morphology of nanocomposites of poly(vinyl chloride) and nano-calcium carbonate. Polym Mater: Sci Eng 2004;91:702.
[83] Xie X-L, Liu Q-X, Li RK-Y, Zhou X-P, Zhang Q-X, Yu Z-Z, et al. Rheological and mechanical properties of PVC/CaCO3 nanocomposites prepared by in situ polymerization. Polymer 2004;45(19):6665.
[84] Xu Y, Malaba D, Huang X, Aguilar-Solis C, Brittain WJ. Polymer-layered silicate nanocomposites by suspension and emulsion polymerizations: PVC-MMT nanocomposites. Polymer Preprints (American Chemical Society, Division of Polymer Chemistry) 43(2); 2002. p. 1312.
[85] Xie X-L, Li RK-Y, Liu Q-X, Mai Y-W. Structure-property relationships of in situ PMMA modified nano-sized antimony trioxide filled poly(vinyl chloride) nanocomposites. Polymer 2004;45(8):2793.
[86] Xu WB, Zhou ZF, Ge ML, Pan WP. Polyvinyl chloride/montmorillonite nanocomposites. Glass transition temperature and mechanical properties. J Thermal Anal Calorim 2004;78(1):91.
[87] Wang D, Parlow D, Yao Q, Wilkie CA. Melt blending preparation of PVC-sodium clay nanocomposites. J Vinyl Additive Technol 2002;8(2):139.
[88] Wan C, Zhang Y, Zhang Y. Structure and properties of polyvinyl chloride-montmorillonite nanocomposites. Zhongguo Suliao 2003;17(11):39.
[89] Kovarova L, Kalendova A, Malac J, Simonik J. PVC/clay nanocomposites via met intercalation: effect of nanocomposite preparation on morphology. Plasty a Kaucuk 2004;41(3-4):6.
[90] Yalcin B, Cakmak M. The role of plasticizer on the exfoliation and dispersion and fracture behavior of clay particles in PVC matrix: a comprehensive morphological study. Polymer 2004;45(19):6623.
[91] Yoo Y, Kim S-S, Won JC, Choi K-Y, Lee JH. Enhancement of the thermal stability, mechanical properties and morphologies of recycled PVC/clay nanocomposites. Polym Bull (Heidelberg, Germany) 2004;52(5):373.
[92] Gong F, Feng M, Zhao C, Zhang S, Yang M. Particle configuration and mechanical properties of poly(vinyl chloride)/montmorillonite nanocomposites via in situ suspension polymerization. Polym Test 2004;23(7):847.
[93] Knudson MI, Powell C. Preparation of polymer nanocomposites from mixture of clay dispersions and polymer dispersions, PCT Int. Appl., Wo, 2002070589; 2002.
[94] Hannecart E, Dupraz A, Petrier C. Process for the fabrication of nanocomposites, Fr. Demande, Fr, 2851567; 2004.
[95] Garcia JL, Koelling KW, Xu G, Summers JW. PVC degradation during injection molding: Experimental evaluation. J Vinyl Additive Technol 2004;10(1):17.
[96] Pozsgay A, Csapo I, Szazdi L, Pukanszky B. Preparation, structure, and properties of PVC/montmorillonite nanocomposites. Mater Res Innovat 2004;8(3):138.
[97] Du J, Wang D, Wilkie CA, Wang J. An XPS investigation of thermal degradation and charring on poly(vinyl chloride)-clay nanocomposites. Polym Degrad Stabil 2002;79(2):319.
[98] Trlica J, Kalendova A, Malac Z, Simonik F, Pospisil L. PVC/clay nanocomposites. 59th ed. Annual technical conference, vol. 2. Society of Plastics Engineers; 2001. p. 2162.
[99] Lepoittevin B, Pantoustier N, Devalckenaere M, Alexandre M, Calberg C, Jerome R, et al. Polymer/layered silicate nanocomposites by combined intercalative polymerization and melt intercalation: a masterbatch process. Polymer 2003;44(7):2033.
[100] Lee M, Lee B-K, Choi K-d. Foam compositions of polyvinyl chloride nanocomposites, PCT Int. Appl., Wo, 2004074357; 2004.
[101] Tudor J, Willington DOH, Royan B. Intercalation of catalytically active metal complexes in phyllosilicates and their application as proprene polymerization catalysts. Chem Commun 1996;17:2031.
[102] Bergman JS, Chen H, Giannelis EP, Thomas MG, Coates GW. Synthesis and characterization of polyolefin-silicate nanocomposites: a catalyst intercalation and in situ polymerization approach. Chem Commun 1999:2179.
[103] Alexandre M, Dubois P, Sun T, Garces JM, Jerome R. Polyethylene-layered silicate nanocomposites prepared by the polymerization-filling technique: synthesis and mechanical properties. Polymer 2002;43(8):2123.
[104] Baker RW. Membrane technology and application. New York: McGraw Hill; 2000.
[105] Hedrick JL, Carter KR, Labadie JW, Miller RD, Volksen W, Hawker CJ, et al. Adv Polym Sci, 1999;141:1.
[106] http://www.unep.org/ozone/sap2002.shtml; 2002.
[107] Kumar V, Schirmer HG. Semi-continuous production of solid-state PET foams. SPE-ANTEC, 53 ed., vol. 2; 1995. p. 2189.
[108] Zeng C, Han X, Lee LJ, Koelling KW, Tomasko DL. Structure of nanocomposite foams. 60th ed. Annual technical conference, vol. 2. Society of Plastics Engineers; 2002. p. 1504.
[109] Strauss W, D'Souza NA. Supercritical CO2 processed polystyrene nanocomposite foams. J Cell Plast 2004;40(3):229.
[110] Nam PH, Maiti P, Okamoto M, Kotaka T, Nakayama T, Takada M, et al. Foam processing and cellular structure of polypropylene/clay nanocomposites. Polym Eng Sci 2002;42(9):1907.
[111] Taki K, Yanagimoto T, Funami E, Okamoto M, Ohshima M. Visual observation of CO2 foaming of polypropylene-clay nanocomposites. Polym Eng Sci 2004;44(6):1004.
[112] Ray SS, Okamoto M. New polylactide/layered silicate nanocomposites. Part 6. Melt rheology and foam processing. Macromol Mater Eng 2003;288(12):936.
[113] Di Y, Iannace S, Di Maio E, Nicolais L. Poly(lactic acid)/organoclay nanocomposites: thermal, rheological properties and foam processing. J Polym Sci, Part B: Polym Phys 2005;43(6):689.
[114] Mitsunaga M, Ito Y, Ray SS, Okamoto M, Hironako K. Intercalated polycarbonate/clay nanocomposites: Nanostructure control and foam processing. Macromol Mater Eng 2003;288(7):543.
[115] Xu G, Lee LJ. PVC Nanocomposite Foams, Internal Communication, 2005.
[116] http://www.favonius.com/soaring/foams/foams.htm; 2004.
[117] http://www.basf.de/basf/html/plastics/englisch/pages/schaum/neopolen.htm; 2004.
[118] http://www.me.dal.ca/~dp_99_1/progress1.htm, 2004.
[119] Martini-Vvedensky JE, Suh NP, Waldman FA. Microcellular closed cell foams and their method of manufacture. US, US 4,473,665; 1984.
[120] www.trexel.com.
[121] Xu J. Reciprocating-screw injection molding machine for microcellular foam. SPE-ANTEC 2001:449.
[122] Jacobsen K, Pierick D. Microcellular foam molding: advantages and application examples. SPE-ANTEC 2000:1929.
[123] Moore S. Foam molding resurgence: sparks competition among processes. Mod Plast 2001(Nov.):23.
[124] Yuan M, Turng L-S, Gong S, Caulfield D, Hunt C, Spindler R. Study of injection molded microcellular polyamide-6 nanocomposites. Polym Eng Sci 2004;44(4):673.
[125] Chandra A, Gong S, Yuan M, Turng L-S, Gramann P, Cordes H. Microstructure and crystallography in microcellular injection-molded polyamide-6 nanocomposite and neat resin. Polym Eng Sci 2004;45(1):52.

[126] Abiko T. Polymer-clay nanocomposites and MuCell foaming. Idemitsu Giho 2003;46(3):281.
[127] Park CB, Baldwin DF, Suh NP. Effect of the pressure drop rate on cell nucleation in continuous processing of microcellular polymers. Polym Eng Sci 1995;35(5):432.
[128] Mahfuz H, Rangari VK, Islam MS, Jeelani S. Fabrication, synthesis and mechanical characterization of nanoparticles infused polyurethane foams. Compos, Part A: Appl Sci Manufact 2004;35A(4):453.
[129] Javni I, Zhang W, Karajkov V, Petrovic ZS, Divjakovic V. Effect of nano and micro-silica fillers on polyurethane foam properties, In: Conference proceedings – polyurethanes expo, Columbus, OH, United States, Sept. 30–Oct. 3; 2001. p. 557.
[130] Kresta JE, Wu JH, Crooker RM. Polyurethane foam containing clay nanocomposite composition with improved thermal insulation. Eur. Pat. Appl., Ep, 1209189; 2002.
[131] Lees GC, Liauw CM, Wilkinson AN, McIntyre A, Burrows D. Montmorillonite flame retardant polyurethane foams and their preparation. Brit. UK Pat. Appl., GB, 2400107; 2004.
[132] Murai S, Kubota Y, Kitano A. Manufacture of polymer nanocomposites containing inorganic fillers with good dispersion, Jpn. Kokai Tokkyo Koho, Jp, 2003261781; 2003.
[133] Sheptalin RA, Koverzanova EV, Lomakin SM, Osipchik VS. Flammability and thermal degradation of a flexible polyurethane foam nanocomposite based on organically modified lamellar aluminosilicate. Plasticheskie Massy 2004(4):20.
[134] Tschritter H, Knoelle G, Oehlert H, Ottow M, Ruebner J. Production of silicic acid/polyurethane nanocomposites from silicic acid/polyol colloids. PCT Int. Appl., WO, 2003016370; 2003.
[135] Krishnamurthi B, Bharadwaj-Somaskandan S, Shutov F, Nano- and micro-fillers for polyurethane foams: effect on density and mechanical properties, In: Conference proceedings – polyurethanes expo, Columbus, OH, United States, Sept. 30–Oct. 3; 2001. p. 239.
[136] Javni I, Zhang W, Karajkov V, Petrovic ZS, Divjakovic V. Effect of nano- and micro-silica fillers on polyurethane foam properties. J Cell Plast 2002;38(3):229.
[137] Kasseh A, Chaouki J, Ennajimi E. Self-foamable organoclay/novolak nanocomposites and process thereof, PCT Int. Appl., Wo, 2004063259; 2004.
[138] Colton JS, Suh NP. The nucleation of microcellular thermoplastic foam with additives. Part I. Theoretical considerations. Polym Eng Sci 1987;27(7):485.
[139] Colton JS, Suh NP. The nucleation of microcellular thermoplastic foam with additives. Part II. Experimental results and discussion. Polym Eng Sci 1987;27(7):493.
[140] Colton JS, Suh NP. Nucleation of microcellular foam: theory and practice. Polym Eng Sci 1987;27(7):500.
[141] Chen L, Straff R, Wang X. Effect of filler size on cell nucleation during foaming process. SPE-ANTEC 2001;59:1732.
[142] Park CB, Behravesh AH, Venter RD. A strategy for the suppression of cell coalescence in the extrusion of microcellular high-impact polystyrene foams. ACS Symp. Ser., vol. 669 (Polymeric Foams); 1997. p. 115.
[143] Shen J, Lee LJ. Effects of carbon nanofibers on polystyrene nanocomposites and foams. 62nd. Annual technical conference, vol. 2. Society of Plastics Engineers; 2004. p. 1836.
[144] Okamoto M, Nam PH, Maiti P, Kotaka T, Nakayama T, Takada M, et al. Biaxial Flow-Induced Alignment of Silicate Layers in Polypropylene/Clay Nanocomposite Foam. Nano Lett 2001;1(9):503.
[145] Ramesh NS, Rasmussen DH, Campbell GA. The heterogeneous nucleation of microcellular foams assisted by the survival of microvoids in polymers containing low glass transition particles. Part 1: mathematical modeling and numerical simulation. Polym Eng Sci 1994;34(22):1685.
[146] Chen L, Wang X, Straff R, Blizard K. Shear stress nucleation in microcellular foaming process. Polym Eng Sci 2002;42:1151–8.
[147] Han JH, Han CD. Bubble Nucleation in Polymeric Liquids. II. Theoretical Considerations. J Polym Sci: Part B: Polym Phys 1990;28:743.
[148] Lee S-T. Shear effects on thermoplastic foam nucleation. Polym Eng Sci 1993;33:418–22.
[149] Zettlemoyer AC. Nucleation. New York: Marcel Dekker; 1969.
[150] Blander M, Katz JL. Bubble nucleation in liquids. AIChE J 1975;21:833–48.
[151] Joshi K, Lee JG, Shafi MA, Flumerfelt RW. Prediction of cellular structure in free expansion of viscoelastic media. J Appl Polym Sci 1998;67(8):1353.
[152] Shafi MA, Joshi K, W. FR, Bubble size distributions in freely expanded polymer foams. Chem Eng Sci 1997;52(4):635.
[153] Gibbs JW. the scientific papers of J. Willard Gibbs. Thermodynamics, vol. I. Woodbridge, CT: Ox Bow Press; 1993.
[154] Fletcher NH. Size effect in heterogeneous nucleation. J Chem Phys 1958;29:572.
[155] Spitael P, Macosko CW, McClurg RB. Block copolymer micelles for nucleation of microcellular thermoplastic foams. Macromolecules 2004;37(18):6874.
[156] Wu S. Polymer interface and adhesion. New York: Marcel Dekker; 1982.
[157] Li H, Lee LJ, Tomasko DL. Effect of carbon dioxide on the interfacial tension of polymer melts. Indus Eng Chem Res 2004;43(2):509.
[158] Jacobasch HJ, Grundke K, Augsburg A, Gietzelt T, Schneider S. Wetting of solids by liquids with low and high viscosity. Prog Coll Polym Sci 1997;105:44 (Trends in Colloid and Interface Science XI).
[159] Snijders EA. Water expandable polystyrene (weps): computational and experimental analysis of bubble growth, Technische Universiteit Eindhoven,Eindhoven, Neth. FIELD URL; 2003.
[160] Gluck G, Hahn K, Gellert R. Production of water-expandable styrene polymers. PCT Int. Appl., Wo, 9948936; 1999.
[161] Crevecoeur JJ, Coolegem JF, Nelissen L, Lemstra PJ. Water expandable polystyrene (WEPS) part 3. Expansion behavior. Polymer 1999;40(13):3697.
[162] Crevecoeur JJ, Nelissen L, Lemstra PJ. Water expandable polystyrene (WEPS) part 2. In situ synthesis of (block)copolymer surfactants. Polymer 1999;40(13):3691.
[163] Crevecoeur JJ, Nelissen L, Lemstra PJ. Water expandable polystyrene (WEPS) part 1. Strategy and procedures. Polymer 1999;40(13):3685.
[164] Pallay J, Berghmans H. Water-blown expandable polystyrene. Improvement of the compatibility of the water carrier with the polystyrene matrix by in situ grafting part II. Influence of compatibilization on the foam quality. Cell Polym 2002;21(1):19.
[165] Pallay J, Kelemen P, Berghmans H, Van Dommelen D. Expansion of polystyrene using water as the blowing agent. Macromol Mater Eng 2000;275:18.